Parameterization of metabolite and macromolecule contributions in interrelated MR spectra of human brain using multidimensional modeling

M. Hoefemann[1,2], C. Bolliger[1,3], D.G. Chong[1,2], J.W. van der Veen[4], R. Kreis[1]

[1]*Departments of Radiology and Biomedical Research, University of Bern, Bern, Switzerland*

[2]*Graduate School for Cellular and Biomedical Sciences, University of Bern, Bern Switzerland*

[3]*Bruker BioSpin AG, Fällanden, Switzerland*

[4]*NIH, NIMH, Magnetic Resonance Spectroscopy Core, Bethesda, MD, USA*

Corresponding author:

Prof. Dr. sc. nat. Roland Kreis,

AMSM, University Bern,

Erlachstrasse 9a,

CH-3012 Bern, Switzerland

Tel: +41-31-632 8174

Email: roland.kreis@insel.ch

published version at https://doi.org/10.1002/nbm.4328

Abstract

Introduction

Macromolecular signals are crucial constituents of short echo-time ^{1}H MR spectra with potential clinical implications in themselves and essential ramifications for the quantification of usually targeted metabolites. Their parameterization, needed for general fitting models, is difficult because of their unknown composition. Here, a macromolecular signal parameterization together with metabolite signal quantification including relaxation properties is investigated by multidimensional modeling of interrelated 2DJ inversion-recovery datasets.

Methods

Simultaneous and iterative procedures for defining the macromolecular background (MMBG) as mono-exponentially or generally decaying signals over TE are evaluated. Varying prior knowledge and restrictions in the metabolite evaluation are tested to examine their impact on results and fitting stability for two sets of three-dimensional spectra acquired with metabolite-cycled PRESS from cerebral gray and white matter locations. One dataset was used for model optimization, also examining the influence of prior knowledge on estimated parameters. The most promising model was applied to a second dataset.

Results

The mono-exponential decay-model appears to be inadequate to represent TE-dependent signal features of the MMBG. TE-adapted MMBG spectra were determined. For a reliable overall quantification of implicated metabolite concentrations and relaxation times, a general fitting model had to be constrained in terms of the number of fitting variables and the allowed parameter space. With such a model in place, fitting precision for metabolite contents and relaxation times was excellent, while fitting accuracy is difficult to judge and bias likely influenced by the type of fitting constraints enforced.

Conclusions

The parameterization of metabolite and macromolecule contributions in interrelated MR spectra has been examined by using multidimensional modeling on complex 2DJ-IR datasets. A tightly restricted model allows fitting of individual subject data with high fitting precision documented in small Cramér-Rao lower bounds, good repeatability values and relatively small spread of estimated concentration and relaxation values for a healthy subject cohort.

Key words

Modeling; multidimensional fitting; simulation of spectra; macromolecules; ^{1}H MR spectroscopy; quantification; prior knowledge; constraints;

published version at https://doi.org/10.1002/nbm.4328

1. Introduction

The quantification of metabolite content in ^{1}H Magnetic Resonance Spectroscopy (MRS) is essential for clinical applications and research investigations[1,2]. Most often, full quantitative evaluation of contributing metabolite characteristics, including not just concentration, but also longitudinal (T_1) and transverse (T_2) relaxation times, is not attempted in clinical studies – let alone for single subjects. Similarly, the macromolecular background (MMBG) is often treated as a nuisance signal to be eliminated rather than quantified and parameterized. This approach is reasonable for spectra acquired in a way to be relatively insensitive to potential pathology-related alterations in relaxation times and as long as the MMBG does not change or is of no interest in disease either. However, this line of attack may miss out on relevant information if in fact relaxation times or the MMBG are altered in disease. The use of separate scans dedicated to determine concentrations, relaxation times and the MMBG is inefficient and a combined use of the data, reminiscent of a fingerprinting approach, is called for and has been proposed before[3–5]. However, concerted multidimensional and multi-parametric modeling poses two major challenges: a) the multitude of interdependent parameters with the danger of overfitting and b) the need for a proper/correct model for fitting that describes the dependence on T_1 and T_2, but also parameterizes the MMBG properly.

In principle, every spectral component adds five parameters[†] to the overall fitting model: the intensity (concentration), a T_1, a T_2, a frequency offset and a phase. Multiple components from the same metabolite are linked by a common concentration (and thus most often a common intensity). Unfortunately, both their longitudinal and transverse relaxation times are not necessarily identical but rather unique for each transition. Hence, based on first principles, metabolites like glutamate (Glu) or N-acetylaspartate (NAA) would add a multitude of fitting parameters to the model, even if the basic spectral features are simulated using the published in-vitro spin system parameters. To make things even more complicated, the MMBG consists of a multitude of unknown contributing molecules with multiple spectral components and with their specific relaxation times, but also potentially including J-couplings rendering the signal evolution with increasing echo time (TE) complex.

It is therefore a non-trivial task to define an appropriate fitting model when fitting a dataset of interrelated spectra, as found for example in the case of 2DJ[3] or inversion recovery (IR)[3] data, or its combination into a 2DJ-IR[3] dataset. The same problem occurs for setting up dictionaries in a fingerprinting approach[6]. While a 2DJ-IR dataset in principle nicely contains all the information needed to determine all relaxation times and concentrations for both metabolites and the MMBG

[†] Six parameters in case of Voigt lines, but the Gauss width, which mostly represents field inhomogeneities, is usually assumed to be identical for all metabolites and thus only adds one parameter overall.

published version at https://doi.org/10.1002/nbm.4328

since it was recorded with various periods of longitudinal and transverse evolution, the large number of parameters to fit renders this non-trivial. The current study was set up to probe the limits of multidimensional fitting of interrelated datasets[3,5,7–9] in terms of the number of independent parameters, but also in terms of whether scalar couplings among components of the MMBG necessitate a fitting model for the MMBG that deviates from the mono-exponential decay that has hitherto been used to describe the TE evolution of MMBG signals[1,3,7].

Given the challenges with the description of the MMBG and the number of fitting parameters needed, accurate knowledge of the metabolite responses for the specific settings is necessary to assemble a valid fitting model. Previous investigations have shown that linear combination model fitting can be based on simulated instead of measured metabolite base spectra[10,11] and different simulation tools are available[12–14]. However, idealized simulations have limited validity. The four-compartment-effect[15,16] can lead to drastic effects at intermediate echo times (e.g. for lactate (Lac) in PRESS[17] or GABA in editing scans[16]). Simulations including real RF pulseshapes and the effect of gradient pulses are lengthy but still feasible for limited steps in multidimensional parameter space. A previous study [18] has shown that the simulation of basis sets should include the effects of the real pulse shapes and limited bandwidths even for the case of short TE and fairly large B_1 amplitude. Therefore, those simulations are included in the fitting models presented here.

The current study was thus set up to contain two parts. In a first step, a 2DJ-IR dataset with intertwined inversion recovery (TI) and TE values with TE limited to values <100 ms was recorded and evaluated. In this part, one focus was set on the challenges of creating a fitting model that is optimal for the number of free fitting parameters and thus the amount of prior knowledge constraints to quantify the metabolite content and to define the MMBG. A second focus lay on investigating whether there is a need for TE-specific MMBG models. In a second part, another 2DJ-IR dataset was recorded from a different cohort of healthy subjects where the developed fitting model was then tested on spectra obtained from white and gray matter volumes. In contrast to the first set, spectra with longer maximal TE values were included, and IR spectra were acquired only for the shortest TE. The presented work gives an overview over the challenges and possibilities of simultaneous fitting of such complex datasets, aiming to quantify metabolite and macromolecular (MM) content as well as relaxation times at 3 T. It presents various fitting options and methods and shows the related results, which are discussed in detail.

published version at https://doi.org/10.1002/nbm.4328

2. Material and Methods

2.1 Data Acquisition

Two different datasets were recorded, one as a straight 2DJ-IR experiment, including general TE and TI combinations, while the other one presents a combination of separate 2DJ and IR datasets to a combined dataset. Both datasets were recorded on a 3T scanner (Trio, Siemens Medical, Erlangen, Germany) with a transmit/receive head coil using a metabolite-cycling PRESS sequence[19,20] with minimized pulse duration (90° Siemens' default sinc pulse, 1.8 ms duration, 8750 Hz bandwith; 180° Siemens' default Mao pulse, 3 ms duration, 2000 Hz bandwidth)) and an initial adiabatic 180° inversion pulse for inversion-recovery scans. Figure 1 specifies values the specific TE and TI combinations of the two datasets.

Dataset 1

10 healthy subjects (30.1 ± 7.9 years; 4 male, 6 female) were examined with a volume of interest (VOI) of 28x28x20 mm^3 centered midline in the occipito-parietal cortex in GM. TE varied from 20 to 95 ms in steps of 5 ms, so that 16 different TE were measured. In one measurement no inversion pulse was used, then three different TIs were measured: 28 ms, 300 ms and 900 ms at each TE, giving 64 spectra in total. The longest TI of 900 ms was chosen to closely null the metabolites, leaving only MM signal. The repetition time (TR), defined as the time between consecutive excitation pulses of the PRESS sequence was 3000 ms for TI of 28 ms and 30 ms and 4000 ms for TI of 900 ms and the non-inverted case, respectively (16 acquisitions per subject, 4000 Hz spectral width, 2048 data points, total acquisition time of 15 min). TR shortening for short TI values allowed reduction in overall scan time with similar recovery time between PRESS and inversion elements and acquisition of a close to fully relaxed spectrum without inversion pulse for better definition of the equilibrium magnetization.

Dataset 2

11 healthy subjects (25.9 ± 4.5 years; 6 male, 5 female; one subject was scanned with 5 repeated measurements) were examined in VOIs of 16x48x17 mm^3 and 25x28x20 mm^3, centered on white matter (WM) in the parietal lobe and on grey matter (GM) in occipito-parietal cortex, respectively. Exact quantitative volume fractions of WM and GM for the ROIs were not determined for lack of MR images suitable for segmentation. Based on other studies, it is estimated that the WM-centered ROI consists of > 80% WM and negligible CSF, while the GM-centered ROI is more evenly distributed with an estimated mean content of 60% GM, 25% WM, and 15% CSF. TE varied from 20 to 307.5 ms in 12.5ms steps, resulting in 24 different TEs. Also, at a constant TE of 20 ms 7 different TIs were

published version at https://doi.org/10.1002/nbm.4328

recorded: 30, 200, 450, 575, 700, 825 and 1200 ms, resulting in 31 spectra in total. TR was set to 2000 ms. 16 acquisitions were averaged per spectrum for GM and 8 for WM in each subject for the non-inverted spectra. For the inverted spectra, 48 acquisitions were averaged in each subject for both WM and GM. Total acquisition time was 24 min for GM and 18 min for WM. This second dataset had already been used in a previous study[3], which focused on modeling methods, with no quantitative results published. Voxel positioning for both datasets is illustrated in Supplements S1.

2.2 Post-Processing

Data processing was performed in MATLAB and cohort averaging in JMRUI[21]. The spectra were automatically aligned, eddy current and phase corrected. For TI=900 ms an additional manual phase correction was necessary. Residual water was removed using Hankel-Lanczos Singular Value Decomposition (HLSVD) filtering[22] (35 components, matrix size 1024). Additional alignment between spectra with different TE was done to correct for a small frequency shift along TE, consistently observed for all subjects. The indicated SNR was calculated from the peak intensity in the experimental spectrum at the frequency position of NAA divided by the standard deviation of the noise in a signal and artefact free region.

2.3 Fitting Procedure

2.3.1 Metabolite basis sets

Metabolite basis sets were simulated in GAMMA[13], using RF pulseshapes and field gradients as used experimentally for the RF pulses. Simulations were adapted to the exact pulse lengths and powers applied in the experiments and were run for every TE individually. In the direction of the 180° pulses, a spatial resolution of 44x44 over a FOV of 55x55 mm^2 was applied for most metabolites (20 points inside the VOI in each direction). For metabolites with complex spin systems (> 5 coupled spins), the resolution had to be reduced to 22x22. For Glucose (Glc), the spatial resolution was neglected due to its complexity (7 spins). For the direction of the 90° pulse that features a large bandwidth, the simulations were not resolved in space and only carried out for the center of the ROI (no offset effects considered). The simulations were run on the high-performance computing cluster UBELIX of the University of Bern.

18 metabolites were included in the fitting model: Aspartate (Asp); Creatine (Cr); γ-aminobutyric-acid (GABA); Glc; Glutamine (Gln); Glu; Glycine (Gly); Glycerophosphorylcholine (GPC); Glutathione (GSH); Lac; myo-Inositol (mI); NAA; N-acetylaspartylglutamate (NAAG); Phosphocholine (PCho);

published version at https://doi.org/10.1002/nbm.4328

Phosphocreatine (PCr); Phosphorylethanolamine (PE); scyllo-Inositol (sI); Taurine (Tau). All metabolites consisting of multiple non-coupled spin systems were divided into sub-patterns for simulation and later use for separate relaxation properties in the cases of isolated methyl groups (see supplemental Tables). Frequency shifts and couplings for the spin systems were taken from Literature[23]. Metabolite content was calculated relative to an assumed amount of total Cr (tCr = Cr plus PCr). For GM the tCr content was set to 8.1 mM, for WM, it was set to 7.8 mM[24].

2.3.2 Development of the fitting model

All model fits and calculation of Cramér-Rao Lower Bounds (CRLB) were performed with FiTAID[3] in frequency domain (domain of χ^2 definition) allowing to fit interrelated datasets with basis spectra defined in time domain and mathematical models for both the T_1 dependence (as function of TI and TR), as well as the T_2 dependence (as function of TE). We created a summed spectrum from all data in dataset 1 to test boundaries and constraints in our fitting model. We summed the data to increase the overall SNR. Phase and frequency offset was fitted simultaneously for the whole dataset (equal for all metabolites and all responses). Metabolite fits started from a Lorentzian broadening of 2 Hz and a Gaussian broadening of 5 Hz.

To probe the limits of our fitting model in terms of the number of independent parameters, the prior knowledge for all model parameters was explored independently in three different ways that we refer to as levels of restriction. Subsequently, we used the most appropriate way to restrict fitting parameters for the evaluation of dataset 2.

- **Restriction level 1:**

  Most metabolites and also their sub-patterns were allowed to vary independently in relaxation time values in wide ranges, which were 625 – 3000 ms for T_1 and 60 – 400 ms for T_2. The following metabolites and sub-patterns were linked to each other in T_1 and T_2: Cr and PCr (methylene and methyl protons separately), mI and sI, as well as PCho and GPC (trimethyl and choline groups separately). For Glc, the concentration ratio between alpha and beta was set to 1:2 and their T_1 and T_2 assumed to be equal. (Total number of parameters to fit: 149.)

- **Restriction level 2:**

  For a more restricted model, the allowed ranges for the relaxation times were reduced to 900 – 2000 ms for T_1 and 100 – 250 ms for T_2 for the following metabolites and sub-patterns with small, coupled molecules (Asp, GABA, Glu, Gln, Glc, Gly, GSH, NAAG (except singlet), PCho and GPC

published version at https://doi.org/10.1002/nbm.4328

(except singlet), PE, Tau). Also, additional links between metabolites and sub-patterns were applied: All sugars were linked to one group (Glc, mI and sI) with identical T_1 and T_2. For the very low concentrated complex patterns of NAAG, the Asp as well as the Glu part was linked to GSH. All other restrictions from level 1 remained active. (Total number of parameters to fit: 143.)

- **Restriction level 3:**

  In the least flexible model, the T_1 and T_2 values were restricted further by linking all metabolite patterns, except for the large singlets. Hence, only the singlets of the creatines, cholines and NAA were allowed to vary independently. All other metabolite patterns were assigned to two groups: One for the sugars (Glc, mI and sI) and one for all others. All other restrictions from level 1 and 2 were also applied. (Total number of parameters to fit: 119.)

2.3.3 Modeling of the MMBG

The MMBG was modeled with 64 equally spaced Voigt lines (spacing Δ=0.05 ppm) between 0.7 and 4.1 ppm with a constant Gaussian broadening of 5 Hz and a starting value for the Lorentzian broadening of 15 Hz. Gaussian broadening and extent of frequency spacing represent a heuristic compromise between minimal number of fitting variables and sufficient freedom to describe the background smoothly. The parameterization of the MMBG as 64 resonance lines, which presents a representation rather than physical modeling, would in principle lead to an enormous number of fitting variables (256=4*64) that would overdetermine the data. Hence, simplifications were imposed on the Gaussian broadenings as explained above, and the relaxation time values. For the latter, it was decided to split the spectrum into multiple parts (with one “peak” each) that would be described with a single T_1 and a single T_2. Instead of using peaks as defined in previous literature, we split peaks at troughs between peaks based on our own data using a preparatory fit step described in Supplements S2. From this initial preliminary fit the lines were assigned to eleven groups to allow subsequent variation of T_1 and T_2 values in the predefined ranges of T_1<400 ms and T_2<35 ms to guarantee a clear separation between MMBG and metabolites.

To test for the extent of deviations from an overall mono-exponential decay model along TE, different models for the MMBG were tested (Figure 2):

i. **Mono-exponential model (MEM):**

   All individual areas of the MMBG lines and grouped T_1s and T_2s were fitted together with the metabolite parameters with the full 2DJ-IR decay model for all spectra in the dataset except for

published version at https://doi.org/10.1002/nbm.4328

those with TE>60 ms at TI=900 ms (very low signal intensity). Fitting parameters for MMBG representation: one area per Voigt line plus one T_1 and one T_2 per group of Voigt lines.

ii. Deviations from mono-exponential model:

Starting from the MEM, keeping all metabolite parameters as well as MMBG T_1s, and T_2s fixed, the areas of all 64 MMBG lines were fitted separately at each TE<65 ms. (For longer TE, MMBG signals were below noise level in the current data sets and their models were thus not adapted but left according to the MEM.) The adjustment of the MMBG at individual TEs was done in two different ways:

- **Method A:** All TIs included, for each TE the spectra from the 4 TIs were fitted together, resulting in 64 free parameters per TE (64 lines, one parameter each).
- **Method B:** Only the metabolite-nulled spectra (TI=900 ms) included; for each TE the spectrum was fitted individually, resulting again in 64 free parameters per TE.

Then for A and B, the MMBG results for all TEs with adapted MMBG amplitudes were copied to the full model preserving their amplitude ratios between all TEs and the whole dataset was fitted again in simultaneous mode, giving the MMBG as well as the metabolite T_1, T_2 and concentrations the possibility to adjust with the new TE-dependent MMBG amplitude model.

2.3.4 Application of resulting models

The summed spectrum over all subjects of dataset 1 was used to test all possible combinations of MMBG models and restriction levels. Then, the model with the highest restriction level (3) and MMBG from Method A were applied to the independent dataset 2 to test its applicability for fitting of individual subject data and transferability to different TE/TI settings. As not all TE values <60 ms of dataset 2 are present in dataset 1, the MMBG was interpolated for those cases. Lorentzian and Gaussian broadenings of the MMBG were held constant.

2.3.5 Statistics

To test for significant differences between metabolite concentration and relaxation times in WM- vs. GM-centered ROIs in dataset 2, a paired t-test was used for normally distributed data. For restricted values reaching the predefined limit in many cases, assuming a normal distribution is not justified and a non-parametric Mann-Whitney U test was used.

published version at https://doi.org/10.1002/nbm.4328

3. Results

An illustration of the measured datasets is given in Figure 1. SNR determined for the subspectrum with TE 20 ms and without inversion was 180 in the cohort average of dataset 1 and 65 in GM and 38 in WM in a typical individual case for dataset 2.

3.1 Modeling and quantification of the MMBG

Pre-fitting the MMBG resulted in a partitioning into 11 groups of MM signal (illustrated in Supplement S2). The patterns for the MMBG as function of TE resulting from the different methods as obtained from dataset 1 are displayed in Figure 3. This includes the results for restriction levels 1 and 3. Allowing the MMBG to adjust for each TE yields deviations from the MEM for both methods (A, B) and all restriction levels. These differences are also visualized in Figure 3. They are particularly evident at ~2.15 ppm for TE >40 ms.

When analyzing the sum spectra of dataset 1, T_1 and T_2 tend to increase along the ppm axis for all three MMBG modeling methods, partially reaching the predefined borders of 35 ms for T_2 and 400 ms for T_1. All estimated relaxation times are provided in supplemental Table S3. Amplitudes of the single lines for a TE of 20 ms in restriction level 3 are stated in supplemental Table S4 for MEM and Method A.

3.2 Modeling of metabolite signals and quantification of their T_1, T_2 and concentrations

Metabolite contents and relaxation times were evaluated for all restriction levels and all MMBG models for dataset 1. The differences in results obtained for different MMBG models are generally very small within each restriction level (see Figure 4 for restriction level 3). Both Method A and B show slightly higher T_1 than MEM for most metabolites. However, differences between the restriction levels are more distinct, not only in relaxation times (mostly explained by stricter boundaries), but also in concentrations as illustrated in Figure 5. For several metabolites, the estimated concentration is lower with tighter restriction. For Gln and Gly for example, it decreases from 4.65 ± 0.1 mM at level 1 to 2.29 ± 0.04 mM at level 3 and from 2.42 ± 0.08 mM to 0.54 ± 0.02 mM, respectively. Detailed results are listed in supplemental Tables S5-S7 and a comparison with literature values is provided in Tables 1-3.

published version at https://doi.org/10.1002/nbm.4328

Figure 6 visually illustrates the fitting results for MEM at restriction levels 1 and 3 at four TE/TI combinations. Fitting performance was good, though not perfect, for all cases; no essential difference between the restriction levels can be visually identified here. χ^2 at the fit minimum increased by 11% from restriction level 1 to level 3.

3.3 Fitting of individual subject data to quantify T_1, T_2 and concentration of metabolites for two VOIs using dataset 2

Fitting of individual subject data from dataset 2 allowed the quantification of metabolite content as well as relaxation times for typical GM and WM locations. A summary of the results is presented in Figure 7 and Tables 1-3. For most parameters, a significant difference between GM and WM was found even though the voxel compositions were not ideally complementary. Detailed results are stated in Supplements S9-S10.

Figure 8 illustrates the fitting results for a representative subject at four TE/TI combinations for both GM and WM. Fitting performance was good for all cases, but residuals showed single non-random features for some spectra that document non-ideal fits and/or non-ideal spectral alignment of the 3D data.

Figure 9 illustrates the consistency in concentration estimates for the 5 repeated measurements in a single subject by plotting the standard deviations (SDs) obtained for those measurements and the mean CRLB from them. Deviations from the mean concentration did not exceed 0.8 mM, while also very small CRLB of $\leq$0.16 mM confirm the excellent precision in parameter estimation. Small SDs and fitting errors were also found for strongly correlated metabolite patterns from the creatines and the cholines. In addition, Figure 9 also juxtaposes the obtained cohort standard deviations for all metabolite concentration estimates. Detailed results for the repeated measurements can be found in Supplements S11-12. Relaxation times showed deviations from the average result of 68 – 150 ms in WM and 26 – 67 ms in GM for T_1 and 7 – 17 ms in WM and 3 – 31 ms in GM for T_2 with CRLB around 20 – 40 ms for T_1 and 2 – 10 ms for T_2.

published version at https://doi.org/10.1002/nbm.4328

4. Discussion

The current work presents a generalization of the previous framework of multidimensional fitting of interrelated MRS datasets. In contrast to Chong et al[3] who have previously explored multidimensional fitting of 2DJ and IR MRS data, the present work uses simultaneous fitting rather than sequential evaluations. Furthermore, it also bases the evaluations on a general combination of 2DJ and IR data where TE and TI are varied independently, whereas earlier, datasets with IR variation for constant TE and TE-variation for a single TI was used. In contrast to An et al[5], who have used simultaneous fitting of a complex model of interrelated data to determine metabolite concentrations and relaxation times at 7 T, we investigated the determination of concentration and relaxation parameters along with the determination of the MMBG. Furthermore, in contrast to any of the previous work, here, it was attempted to determine model-free MMBG spectra for multiple TEs from single datasets.

In principle, the described tool and acquired datasets allow for determination of metabolite relaxation and concentration parameters together with a subject-specific MMBG signal from a single examination. However, it was found that the fit problem is clearly too complex for a single unrestricted fit with all parameters just restrained into the physically possible ranges without further strict restraints and relations imposed by plausibility (or physical and physiological common sense) even though the data matrix of up to 16000 points[‡] would theoretically allow to determine a very large number of fitting parameters.

Therefore, the current work, besides describing the data and fitting program, focused on two main questions: 1st whether there is a need to go beyond an exponential decay model for the MMBG signal, and 2nd which fitting restraints have to be enforced for an optimal compromise between maximal information content from the fit and acceptable robustness of the obtained fit parameters. In addition, the methods were then employed to determine concentrations and relaxation times for an independent spectral dataset from WM and GM dominated ROIs in a further cohort of volunteers.

Modeling the MMBG

Modeling the MMBG with equally-spaced Voigt lines with Gaussian and Lorentzian broadening is a common method to represent[25] and parameterize the MMBG. Here, the representation serves to describe the MMBG signal in a 2DJ-IR data model, including longitudinal and transverse[§] relaxation times that were allowed to vary in eleven groups of MM signals. The detailed information in the

[‡] 16000 =64 x 250, derived from 64 spectra with differing acquisition parameters and around 250 spectral points in the spectral window of interest

[§] limited significance for estimated T_2s for the non-MEM cases

published version at https://doi.org/10.1002/nbm.4328

supplements allows readers to construct the MMBG spectra found in this work to be used further in their own research. However, we would like to caution that with the known shortcomings of our approach (see below) they should not be considered a gold standard.

Given that some MM signal components are known to feature signal evolution due to J-coupling and given that none of the individual Voigt lines represents a single molecular entity, the signal behavior along TE cannot be accurately described as a mono-exponential decay. The described Methods A and B allow adjustment of the relative signal intensities for each TE and the results showed clear deviations from the mono-exponential decay model. These differences in the MMBG are evident from the estimated MMBG spectra in Figure 3. The main deviations from MEM are similar for Methods A and B and also at both restriction levels, but there are differences in the details, though it is not obvious which treatment is better. It is striking that the potential to adapt relative signal amplitudes at different TEs seems to clearly lead to more structure in the MMBG, which is otherwise only seen at higher B_0. However, this effect is likely introduced artificially by grouping the MMBG with identical T_2 within the single groups. Overall, there are some strong deviations from MEM for longer TEs at certain frequencies, in particular at 0.9 and 2.1 ppm. The J-couplings between several MM signal components have originally been reported by Behar et al.[26]. Figure 3 includes an indication of some of those couplings. However, J-coupling would lead to stronger signal disappearance at the coupling partners' resonance frequencies than expected based on T_2 only. What is seen at 2.1 ppm is more retained signal at TE 40 to 60 ms, rather than less, while at 0.9 ppm such stronger signal decay is indeed observed to some extent.

One major challenge with modeling the MMBG in this way is the enforced prior knowledge on the metabolite signals. To allow the individual resonance amplitudes of the MMBG to adjust at each TE, the overall 2DJ-IR model cannot reasonably be used and the parameters describing the metabolites have to be held constant at the values obtained with the MEM. Suggesting that the MEM model of the MMBG is not quite adequate also means that the metabolite content is somewhat biased. If the MMBG is adjusted at each TE to a biased metabolite model, this bias is inversely also transferred to the MMBG. However, not using any mono-exponential model for the MMBG in the first place in the overall model would cause the loss of any prior knowledge on the relaxation times of the MM components and hence give the MMBG unwanted freedom to adapt.

This problem becomes clearer when comparing the MMBG models of restriction levels 1 and 3 in Figure 3. Due to the different results for the metabolites in the first fit (MEM), also the MMBG models differ for MEM and subsequently for Models A and B.

published version at https://doi.org/10.1002/nbm.4328

Assembling a fitting model to quantify metabolite concentrations and relaxation times T_1 and T_2

For many metabolites, the differences in estimated concentrations between the restriction levels are quite high, documenting that the estimated relaxation times have a large impact on the concentration results. This is particularly true for those metabolites that had to be restricted in terms of their relaxation times as no stable fitting had been achieved for T_1 and/or T_2 without restrictions. As no ground truth prior knowledge is available in the literature for the relaxation times for any metabolite and metabolite subgroup, it is not possible to draw clear-cut conclusions in terms of fitting accuracy.

However, plausibility of the results can be examined by comparison to literature values (Tables 1-3 [24,27–31]). Results are comparable in many cases. For the metabolites showing a higher difference between the restriction levels, such as GABA, Gln, Glc or Tau, their concentration estimates are closer to literature values for models with higher parameter restrictions, hinting that with an increasing number of fit parameters the data was partially overfitted.

The estimation of the relaxation times T_1 and T_2 for individual metabolite sub-patterns proved to be difficult in complex models. Many parameters reached the predefined borders for the restriction levels 1 and 2 such that no meaningful fit was possible for those metabolites (and thus all metabolites with overlapping spectral patterns). To avoid bias caused by these instabilities, restriction level 3 was introduced that allows almost no variation in relaxation times between the metabolites. In this case, the relaxation times consistently remained within the allowed ranges, as the signal behavior of the signal-intense metabolites dominates the overall fit. It is clear however, that this method is also biased, because in reality, variations between the relaxation times of different metabolite patterns do exist. Due to the enforced link between those parameters, not only the estimated parameters for the low-concentration metabolites but also those for the dominating metabolites are biased and the fit of the relaxation times is a compromise for all connected patterns.

It is striking that for the singlets, T_1 is quite constant over the different levels of restriction, while for Glu and mI they are higher with more restriction. The T_1 of Glu for example is free to adjust in level 1 and 2, showing an almost identical T_1 of 1419 ms and 1437 ms. For level 3, where several other patterns are linked to the T_1 of Glu, it increases to 1664 ms, which is much higher than literature values (Table 2).

The level of restriction also has an influence on the estimated T_2 parameters. E.g. for Gln, the high freedom model found quite a low T_2 of 90 ms (similar to literature values in Ref[29]) while with linking to other patterns this value increased to 189 ms.

published version at https://doi.org/10.1002/nbm.4328

Application of the fitting model to individual subject GM and WM data from dataset 2 with different TE/TI combinations

Fitting of individual subject data proved to be successful with the chosen model despite lower SNR, as proven by the fact that individual fitting results on average were close to the fits of the averaged spectrum with small SDs over the cohort. In addition, significant differences between GM- and WM-dominated ROIs could be found. Furthermore, the five repeated measurements in one subject (Figure 9) showed good repeatability in quantification of metabolite content and determination of relaxation times for many metabolites. Furthermore, comparison to the CRLB, which stands for the minimal variation based on the fitting model and SNR alone, show that deviations are in a reasonable range around the mean value. As expected, SDs over the cohort are larger, but again indicate that the nature of the interrelated datasets guarantees precise definition of the parameter estimates (at least with the restriction level 3). This even extends to the closely related Cr/PCr and PCho/GPC patterns.

While CRLB, repeatability and SD over cohorts are all indicators for precision, comparison to literature values from earlier studies with mostly traditional methods may point at the accuracy of the generalized scheme.

Table 1 provides a comparison between estimated tissue contents for WM and GM from dataset 2 and the GM values from dataset 1 (for the subsequently chosen fit model with restriction level 3, MMBG method A) compared to literature studies, which also included data for GM- and WM-weighted VOIs ([24,27]). For most metabolites, the values are in fair agreement, though literature values themselves do often not agree very well. The GM tissue contents also differ substantially for a few of the metabolites as estimated from the two datasets with differing acquisition schemes. It appears that those from dataset 1 are somewhat closer to what can be expected from the literature (in particular for GABA, Glu, and NAAG); possibly hinting that the generalized combinations of TE/TI are to be preferred. There are also striking differences in T_2 between datasets; T_2s are longer for all metabolite groups for dataset 2, which includes recordings with much longer TE than in the scheme for dataset 1 (Tables 2-3).

For the concentrations, it has to be noted that tCr was used as reference, which has a different concentration for WM and GM. Hence the significant WM/GM differences and also comparison to literature is all potentially biased by the chosen reference values for tCr (particularly noteworthy if comparing to the values published in Ref.[27]). No reference is involved when comparing relaxation times to literature values or between WM and GM. While general trends for relaxation times between metabolites are well reproduced in this study, it is striking that for most of them the currently obtained values are considerably longer than what is found in literature, both for T_1 and T_2.

published version at https://doi.org/10.1002/nbm.4328

Given that a similar difference had been found at 1.5 T when comparing the results from a combined modeling in Ref.[7] with traditional approaches, it could be that simultaneous adaptation of the MMBG with determination of metabolite relaxation times favors long metabolite relaxation times. Similarly in the past, relaxation times have often been determined for the full spectral pattern of metabolites, hence arriving at a compromise of real relaxation rates of the singlets from methyl groups and those from the rest of the metabolite, where the true relaxation rates are usually smaller for the methyl groups. In the current study (and in Ref.[7]) but also in Ref.[29] separate relaxation times from the methyl parts of the metabolite patterns have been estimated.

Limitations and Perspectives

This study has clear limitations.

SNR: The conclusions in terms of favoring more restrictive prior knowledge constraints and narrower parameter ranges are valid for the currently available data with limited SNR for individual subspectra. As the datasets consist of many combinations of TE and TI, increasing the number of acquisitions per subspectrum was not feasible as it would require even more scanning time. However, one could explore the use of less TE/TI combinations in favor of better SNR for each of those spectra. The results of Bolliger et al[4] show that indeed for many metabolites combinations with few TE combinations (in 2DJ) are better than a uniform spread of acquisition time between many combinations. However, any selection of particular parameters will only optimize estimation of a subset of parameters. Alternatively, the use of a phased array coil (rather than the transmit/receive head coil used, which was a compromise towards higher transmit fields rather than better sensitivity), larger ROIs and of course higher B_0 fields would allow to obtain overall better SNR data that may well provide a better basis to prevent erratic results for some of the less pronounced metabolite signals and thus also better definition of the TE-specific MMBG patterns.

Frequency shifts: It was challenging to align all spectra properly, given that hardware drifts or subject motion can lead to frequency drifts on one hand and that slowly-decaying eddy currents can also appear like small frequency shifts between different TE acquisitions. On top, alignment of spectra using the water signal in metabolite-cycled scans can - though superior to alignment of water suppressed data in most cases - also lead to systematic problems for parameter combinations that either lead to low water signal overall or that give different weights for water signals from different water compartments (WM/GM/CSF/myelin water) with potentially different center frequency. A systematic frequency shift between spectra of specific parameter combinations was evaluated for the summed data from all subjects and then corrected for each individual data set. Still, this correction may not be appropriate for all data. In addition, frequency shifts between metabolite

published version at https://doi.org/10.1002/nbm.4328

patterns were not allowed in fitting, thus relying on appropriateness of the shift parameters from in-vitro literature.

Restrictions in parameter space: The choice of the boundaries for the allowed parameter space was arbitrary and results are clearly influenced if parameters are limited by these boundary conditions. Hence it was one of the aims of this work to arrive at fitting conditions that would not or rarely yield parameters at the boundaries, but even in the finally used configuration this could not be prevented completely (e.g. for some T_2 values in the WM case).

MMBG model: A general model-free description of the MMBG was chosen to represent the MMBG spectrum for different TEs (though subdivided arbitrarily into partitions with equal relaxation times). Given that some information on J-couplings is available from early work of Behar et al. and some recent suggestions exist on the underlying constitution the MMBG [32], it may be promising to compose the MMBG signal into single constituents similarly to the metabolites, but at present that would also introduce some arbitrary selections.

5. Conclusions

The parameterization of metabolite and macromolecule contributions in interrelated MR spectra has been examined by using multidimensional modeling of complex 2DJ-IR datasets. The modeling was successful with minimal residuals for most subspectra and definition of TE-specific MMBG patterns. However, with the available SNR-limited datasets, no unique solutions as to defining which parameter-restriction is optimal could be obtained. The study clearly showed that FiTAID provides the appropriate framework for simultaneous evaluation of a large multidimensional fit model to simultaneously determine metabolite contents, metabolite T_1 and T_2 values, as well as the TE-specific MMBG parameters. However, it became also very clear that the SNR in generally achievable datasets is too low for a general unbiased solution. Thus, arbitrary sequential fit strategies and choice of allowed parameter spaces is still needed even if the general fit problem can be formulated and technically solved.

Based on the currently available datasets, deviations of the previously used mono-exponential signal decay behavior for MMBG have been shown. Different methods to describe the MMBG signals have been proposed and lead to somewhat different results, but do not influence the concurrent estimation of metabolite contents much.

Using one of the non-mono-exponential decay models for MMBG definition and a largely restricted parameter model for metabolite relaxation constants, it was possible to fit metabolite contents and relaxation times with high precision as documented by the CRLB, reproducibility of estimates in a

published version at https://doi.org/10.1002/nbm.4328

single subject and small SDs of estimates over a cohort of healthy subjects. This is very promising for the detection of pathologic changes in groups of patients or even for single subjects. Estimated tissue contents and relaxation constants for white and gray matter locations are provided for a large number of metabolites. However, lack of ground truth values for establishing the details of the fit model and the potential to overfitting the data when the model is not strongly restricted, limits the potential for trustworthy interpretation of the results in absolute values.

Acknowledgement

This work was supported by the Swiss National Science Foundation (320030-156952 and 320030-175984).

published version at https://doi.org/10.1002/nbm.4328

List of Figure Captions

Figure 1 – *Presentation of the measured data as averages over all subjects for the two setups, also illustrating the TE and TI combinations of dataset 1 (above) and dataset 2 (below): Dataset 1 consists of 64 spectra, dataset 2 of 31. While dataset 2 only includes inversion recovery spectra for the shortest TE of 20 ms, dataset 1 contains all possible combinations of 16 TE and 4 TI values.*

Figure 2 – *Illustration of the different modeling methods used to define the MMBG. Starting from the mono-exponential decay model MEM, two different models are constructed by allowing adaptation of individual MMBG constituent resonances to the spectra obtained at the different TE values, using either all TI spectra (Method A) or only the metabolite-nulled TI spectra (Method B). The figure also includes the initial fit step to partition the MMBG into subcomponents with equal relaxation times and shows the last step to arrive at metabolite values with the adapted MMBG models.*

Figure 3 – Presentation of the *resulting MMBG for TE 20 to 60 ms for MEM (no adjustments at individual TEs) and the Methods A and B (see text and Figure 2). Results are displayed for restriction level 1 (left) and 3 (right). In both cases, Methods A and B yield some intensity differences with respect to the MEM model that are included as difference spectra. Known couplings for MM resonances from Literature* [26] *are indicated (red, green and yellow arrows).*

Figure 4 – *Presentation of estimated metabolite parameters as function of the choice of MMBG model, displayed for restriction level 3 (stricter limits and most relaxation times linked). Above: Concentrations of metabolites shows only small differences between MMBG models. Below: Relaxation times T_1 and T_2 remain almost constant for the different MMBG models.*

Figure 5 -Presentation of estimated metabolite parameters as function of *the choice of restriction level for metabolite evaluation, averaged over the three modeling methods for the MMBG. Above: Concentrations of metabolites (with indication of standard deviation over the three MMBG models) change with restriction level for most metabolites. Below: Relaxation times T_1 and T_2 with different permitted parameter ranges showed stabilization of estimated parameters for restriction level 3.*

Figure 6 - *Illustration of fitting results for dataset 1 for restriction level 1 (above) and 3 (below) with MEM MMBG for four different combinations of TE and TI: No inversion at TE 20 ms and 60 ms and metabolite-nulling inversion at TI 900 ms for the same TEs. Measured data is displayed in black, fit in dotted blue lines and residues in red. Fitting performance was good in all cases; no essential difference between the restriction levels can be spotted by visual inspection.*

published version at https://doi.org/10.1002/nbm.4328

Figure 7 – *Results and standard deviations from fitting of individual subject data of dataset 2. Above: Results for concentration with indication of significant differences between GM and WM metabolite contents. Below: Results for relaxation times T_1 and T_2. For most concentrations and relaxation times, the differences between estimated values in GM and WM were found to be significant.*

Figure 8 - *Illustration of fitting results for spectra of dataset 2 for a representative subject, GM (above) and WM (below) data for four different combinations of TE and TI are included: No inversion at TE 20 ms and 145 ms and the data for TI of 200 ms and 700 ms, each for TE 20 ms. Experimental data is displayed in black, fit in dotted blue lines and residues in red. Fitting performance was equally good for all cases as judged by visual inspection.*

Figure 9 – *Illustration of the repeatability estimation for metabolite contents from repeated measurements in the GM and WM VOIs in a single subject plotted along with the mean CRLB from these 5 measurements and in comparison with the cohort standard deviations obtained from 11 measurements in healthy subjects. As expected the CRLBs are mostly smaller than repeatability estimates and they are again smaller than the variation over the cohort, which is substantially larger for some metabolites in particular for the lower SNR data in WM, which may be substantially influenced by the variable extent of GM contributions between subjects.*

published version at https://doi.org/10.1002/nbm.4328

List of Table Captions

Table 1 -*Comparison of the metabolite concentration estimates with Literature values. For dataset 1, averaged over all MMBG methods, most metabolites are in good agreement. Those metabolites that showed quite a high concentration in this study, approach literature values with increasing restriction level. For dataset 2, in most cases, concentration results are in valid agreement with Literature GM and WM values. Comparing the absolute numbers, one needs to consider the different amount of tCr for GM in the different studies, which was used here as an internal reference and therefore influences all metabolite concentrations. The results from dataset 1 with the later chosen model (level 3, Method A) are in good comparison with dataset 2 for most metabolites.*

Table 2 – *Comparison of the metabolite T_1 relaxation times estimates with Literature values. For dataset 1, the singlets show quite constant values, while the other patterns show increasing T_1 with higher restriction level, also exceeding the values stated in Literature. For dataset 2 differences between WM and GM are as expected from Literature, though also above those values in some cases.*

Table 3 – *Comparison of the metabolite T_2 relaxation time estimates with Literature values. For dataset 1, the level of restriction also shows an effect mostly on the non-singlet patterns. Most values are in good agreement with the Literature values. For dataset 2, the T_2 of the main group of metabolites and the NAA singlet reached the predefined upper borders in the summed fitting and also for most individuals in WM. In total, T_2 values in dataset 2 showed higher values than in Literature, and also in dataset 1 in some cases compared with the results from the later chosen model (level 3, Method A).*

published version at https://doi.org/10.1002/nbm.4328

References

1. Wilson M, Bizzi A, Cudalbu C, et al. Methodological consensus on clinical proton MRS of the brain : Review and recommendations. *Magn Reson Med*. 2019;82:527–550. doi:10.1002/mrm.27742
2. Oz G, Alger JR, Barker PB, et al. Clinical Proton MR Spectroscopy in Central Nervous System Disorders. *Radiology*. 2014;270(3):658–679.
3. Chong DGQ, Kreis R, Bolliger CS, Boesch C, Slotboom J. Two-dimensional linear-combination model fitting of magnetic resonance spectra to define the macromolecule baseline using FiTAID, a Fitting Tool for Arrays of Interrelated Datasets. *MAGMA*. 2011;24(3):147–164. doi:10.1007/s10334-011-0246-y
4. Bolliger CS, Chong DG, Slotboom J, Boesch C, Kreis R. Modeling of 3-dimensional MR spectra of human brain: Simultaneous determination of T1, T2, and concentrations based on combined 2DJ inversion-recovery spectroscopy. In: *Proceedings of the 18th scientific meeting of ISMRM and ESMRMB, Stockholm, Sweden, 2010. p 3325*.
5. An L, Li S, Shen J. Simultaneous determination of metabolite concentrations, T_1 and T_2 relaxation times. *Magn Reson Med*. 2017;78(6):2072–2081. doi:10.1002/mrm.26612
6. Kulpanovich A. What is the optimal schedule for multiparametric MRS ? A magnetic resonance fingerprinting perspective. *NMR Biomed*. 2019;e4196:1–12. doi:10.1002/nbm.4196
7. Kreis R, Slotboom J, Hofmann L, Boesch C. Integrated data acquisition and processing to determine metabolite contents, relaxation times, and macromolecule baseline in single examinations of individual subjects. *Magn Reson Med*. 2005;54(4):761–768. doi:10.1002/mrm.20673
8. Adalid V, Döring A, Kyathanahally SP, Bolliger CS, Boesch C, Kreis R. Fitting interrelated datasets: metabolite diffusion and general lineshapes. *MAGMA*. 2017;30(5):429–448. doi:10.1007/s10334-017-0618-z
9. Bolliger CS, Boesch C, Kreis R. On the use of Cramér-Rao minimum variance bounds for the design of magnetic resonance spectroscopy experiments. *Neuroimage*. 2013;83:1031–1040. doi:10.1016/j.neuroimage.2013.07.062
10. Cudalbu C, Cavassila S, Rabeson H, Ormondt D van, Graveron-Demilly D. Influence of measured and simulated basis sets on metabolite concentration estimates. *NMR Biomed*. 2007;21:627–636. doi:10.1002/nbm
11. Wilson M, Davies NP, Sun Y, et al. A comparison between simulated and experimental basis sets for assessing short-TE in vivo1H MRS data at 1.5 T. *NMR Biomed*. 2010;23(10):1117–1126. doi:10.1002/nbm.1538
12. Starčuk Z, Starčuková J. Quantum-mechanical simulations for in vivo MR spectroscopy: Principles and possibilities demonstrated with the program NMRScopeB. *Anal Biochem*. 2017;529:79–97. doi:10.1016/j.ab.2016.10.007
13. Smith SA, Levante TO, Meier BH, Ernst RR. Computer Simulations in Magnetic Resonance. An Object-Oriented Programming Approach. *J Magn Reson Ser A*. 1994;106(1):75–105.
14. Soher BJ, Semanchuk P, Todd D, Steinberg J, Young K. VeSPA: Integrated applications for RF pulse

published version at https://doi.org/10.1002/nbm.4328

design, spectral simulation and MRS data analysis. In: *Proceedings of the 19th Annual Meeting of ISMRM, Montreal, Canada, 2011. p. 1410*.

15. Maudsley AA, Govindaraju V, Young K, et al. Numerical simulation of PRESS localized MR spectroscopy. *J Magn Reson*. 2005;173(1):54–63. doi:10.1016/j.jmr.2004.11.018
16. Kaiser LG, Young K, Meyerhoff DJ, Mueller SG, Matson GB. A detailed analysis of localized J-difference GABA editing: theoretical and experimental study at 4 T. *NMR Biomed*. 2007;21:22–32. doi:10.1002/nbm
17. Lange T, Dydak U, Roberts TPL, Rowley HA, Bjeljac M, Boesiger P. Pitfalls in Lactate Measurements at 3T. *AJNR Am J Neuroradiol*. 2006;27:895–901. doi:10.1007/BF02386831
18. Hoefemann M, Veen JW Van Der, Kreis R. Quantitative evaluation of systematic bias in clinical MRS introduced by the use of metabolite basis sets simulated with ideal RF pulses. In: *Proceedings of the 26th scientific meeting, International Society for Magnetic Resonance in Medicine, Paris, France, 2018, p 1313*.
19. Macmillan EL, Chong DGQ, Dreher W, Henning A, Boesch C, Kreis R. Magnetization exchange with water and T1 relaxation of the downfield resonances in human brain spectra at 3.0 T. *Magn Reson Med*. 2011;65(5):1239–1246. doi:10.1002/mrm.22813
20. Dreher W, Leibfritz D. New method for the simultaneous detection of metabolites and water in localized in vivo1H nuclear magnetic resonance spectroscopy. *Magn Reson Med*. 2005;54(1):190–195. doi:10.1002/mrm.20549
21. Stefan D, Di Cesare F, Andrasescu A, et al. Quantitation of magnetic resonance spectroscopy signals: The jMRUI software package. *Meas Sci Technol*. 2009;20:104035. doi:10.1088/0957-0233/20/10/104035. doi:10.1088/0957-0233/20/10/104035
22. KU Leuven BioMed SPID package: https://homes.esat.kuleuven.be/~biomed/software.php#SpidGUI.
23. Govindaraju V, Young K, Maudsley AA. Proton NMR chemical shifts and coupling constants for brain metabolites. *NMR Biomed*. 2000:129–153.
24. van de Bank BL, Emir UE, Boer VO, et al. Multi-center reproducibility of neurochemical profiles in the human brain at 7T. *NMR Biomed*. 2015;28(3):306–316. doi:10.1002/nbm.3252
25. Novikov DS, Kiselev VG, Jespersen SN. On modeling. *Magn Reson Med*. 2018;79(6):3172–3193. doi:10.1002/mrm.27101.On
26. Behar KL, Rothman DL, Spencer DD, Petroff OAC. Analysis of macromolecule resonances in 1H NMR spectra of human brain. *Magn Reson Med*. 1994;32(3):294–302. doi:10.1002/mrm.1910320304
27. Pouwels PJW, Frahm J. Regional metabolite concentrations in human brain as determined by quantitative localized proton MRS. *Magn Reson Med*. 1998;39(1):53–60. doi:10.1002/mrm.1910390110
28. Mekle R, Mlynárik V, Gambarota G, Hergt M, Krueger G, Gruetter R. MR spectroscopy of the human brain with enhanced signal intensity at ultrashort echo times on a clinical platform at 3T and 7T. *Magn Reson Med*. 2009;61(6):1279–1285. doi:10.1002/mrm.21961
29. Wyss PO, Bianchini C, Scheidegger M, et al. In vivo estimation of transverse relaxation time constant

published version at https://doi.org/10.1002/nbm.4328

(T2) of 17 human brain metabolites at 3T. *Magn Reson Med*. 2018;80(2):452–461. doi:10.1002/mrm.27067

30. Mlynarik V, Gruber S, Moser E. Proton T1 and T2 relaxation times of human brain metabolites at 3 Tesla. *NMR Biomed*. 2001;14(5):325–331. doi:10.1002/nbm.713

31. Träber F, Block W, Lamerichs R, Gieseke J, Schild HH. 1H Metabolite Relaxation Times at 3.0 Tesla: Measurements of T1 and T2 Values in Normal Brain and Determination of Regional Differences in Transverse Relaxation. *J Magn Reson Imaging*. 2004;19(5):537–545. doi:10.1002/jmri.20053

32. Borbáth T, Manohar SM, Henning A. Towards a Fitting Model of Macromolecular Spectra : Amino Acids. In: *Proceedings of the 27th annual meeting of ISMRM, Montreal, Canada, 2019, p 1068*.

published version at https://doi.org/10.1002/nbm.4328

Table 1

Concentration [mM]	This study						Literature				
	Dataset 1 (GM)				Dataset 2		Van de Bank et al. 2015 (21)		Pouwels and Frahm 1998 (24)		Mekle et al. 2009 (25)
	Level 1, MMBG avg	Level 2, MMBG avg	Level 3, MMBG avg	Level 3, Method A	WM	GM	WM	GM	WM	GM	WM
Asp	3.70	3.60	2.78	2.76	1.24 ± 0.55	2.83 ± 0.32	2.0	2.0	-	-	3.1
Cr	6.82	6.66	6.85	6.86	5.42 ± 0.58	6.26 ± 0.48	-	-	-	-	5.8
GABA	0.88	1.16	1.24	1.18	1.15 ± 0.41	2.12 ± 0.42	1.3	1.3	-	-	2.5
Glc	2.71	1.13	1.67	1.62	3.33 ± 0.60	1.77 ± 0.51	-	-	-	-	1.4
Glu	8.42	9.09	9.02	9.02	7.92 ± 0.43	10.99 ± 0.55	7.2	9.4	6.0 – 7.0	8.2 – 8.6	8.9
Gln	4.65	4.34	2.29	2.28	2.17 ± 0.52	3.96 ± 0.46	2.4	5.2	1.5 – 2.2	3.8 – 4.4	1.6
GSH	1.99	2.23	1.30	1.30	1.30 ± 0.20	1.43 ± 0.13	1.2	1.2	-	-	1.4
Gly	2.42	1.05	0.54	0.53	0.00 ± 0.00	0.47 ± 0.18	-	-	-	-	-
GPC	0.39	0.33	0.31	0.30	1.22 ± 0.15	0.08 ± 0.07	-	-	-	-	-
Lac	0.50	0.40	0.47	0.46	0.53 ± 0.23	0.51 ± 0.20	0.9	0.8	-	-	-
mI	4.61	5.61	5.74	5.73	8.18 ± 1.00	6.11 ± 0.63	6.2	6.4	3.1 – 4.1	4.1 – 4.3	5.3
NAA	7.97	8.13	8.63	8.61	10.38 ± 1.00	9.81 ± 0.40	-	-	7.8 – 8.1	7.7 – 9.2	11.2
NAAG	2.00	1.17	1.08	1.07	3.59 ± 0.65	2.09 ± 0.39	-	-	1.5 – 2.7	0.5 – 1.4	1.0
PCr	1.28	1.44	1.25	1.24	2.38 ± 0.58	1.84 ± 0.48	-	-	-	-	2.2
PCho	0.62	0.71	0.65	0.66	0.02 ± 0.04	0.92 ± 0.11	-	-	-	-	-
PE	1.11	1.08	1.29	1.25	2.59 ± 0.66	1.92 ± 0.51	1.4	1.6	-	-	2.2
sI	0.28	0.36	0.38	0.39	0.46 ± 0.10	0.33 ± 0.06	0.3	0.3	-	-	0.4
Tau	2.77	2.27	1.18	1.21	0.49 ± 0.77	1.70 ± 0.24	-	-	-	-	1.4
GPC + PCho	1.01	1.04	0.96	0.96	1.24 ± 0.19	1.00 ± 0.18	1.9	1.3	1.6 – 1.8	0.9 – 1.4	1.1
Cr + PCr	8.10	8.10	8.10	8.10	7.8 ± 1.16	8.1 ± 0.96	7.8	8.1	5.5 – 5.7	6.4 – 6.9	8.0
NAA + NAAG	9.97	9.30	9.71	9.68	13.97 ± 1.65	10.90 ± 0.79	13.6	12.1	-	-	12.2
Glc + Tau	5.48	3.40	2.85	2.83	3.82 ± 1.37	3.47 ± 0.65	1.3	2.3	-	-	2.8

published version at https://doi.org/10.1002/nbm.4328

Table 2

T_1 [ms]	This study						Literature		
	Dataset 1 (GM)				Dataset 2		Mlynarik et al. 2001 [27]		Träber et al. 2004 [28]
	Level 1, MMBG avg	Level 2, MMBG avg	Level 3, MMBG avg	Level 3, MMBG Method A	WM	GM	WM	GM	WM and GM
Cr / PCr CH_2	1131	1191	1281	1289	1039 ± 93	1191 ± 92	870	970	760 – 1020
Cr / PCr CH_3	1728	1775	1740	1737	1692 ± 132	1606 ± 53	1240	1460	1110 - 1470
Glu	1419	1437	1664	1696	1562 ± 128	1714 ± 103	1170	1270	-
mI	1278	1383	1461	1491	1240 ± 82	1325 ± 41	1010	1230	980 - 1360
NAA	1050	1036	1664	1696	1562 ± 128	1714 ± 103	-	-	-
NAA singlet	1606	1692	1583	1589	1608 ± 98	1755 ± 115	1350	1470	1340 - 1390
GPC / PCho trimethyl	1289	1320	1450	1461	1336 ± 100	1358 ± 86	1080	1300	1140 - 1150

published version at https://doi.org/10.1002/nbm.4328

Table 3

T_2 [ms]	This study						Literature					
	Dataset 1 (GM)				Dataset 2		Mlynarik et al. 2001 [27]		Träber et al. 2004 [28]		Wyss et al. 2018 [26]	
	Level 1, MMBG avg	Level 2, MMBG avg	Level 3, MMBG avg	Level 3, MMBG Method A	WM	GM	WM	GM	WM	GM	WM	GM
Cr / PCr CH_2	113	117	110	110	145 ± 11	137 ± 4	152 ± 7	116 ± 9	127	121	129 ± 13	112 ± 18
Cr / PCr CH_3	170	178	170	170	220 ± 13	202 ± 7	156 ± 20	152 ± 7	178	162	166 ± 11	144 ± 17
Glu	193	181	189	190	250 ± 4	205 ± 11	-	-	-	-	124 ± 37	122 ± 32
Gln	90	100	189	190	250 ± 4	205 ± 11	-	-	-	-	168 ± 33	99 ± 21
mI	269	192	175	175	149 ± 18	229 ± 23	-	-	-	-	161 ± 37	229 ± 105
NAA R	295	313	189	190	250 ± 4	205 ± 11	-	-	-	-	310 ± 33	229 ± 38
NAA singlet	356	381	295	298	400 ± 0.5	349 ± 29	295 ± 29	247 ± 19	301	247	343 ± 34	263 ± 43
NAAG singlet	107	199	189	190	250 ± 4	205 ± 11	-	-	-	-	185 ± 22	107 ± 19
GPC / PCho trimethyl	164	174	185	187	269 ± 18	314 ± 21	187 ± 20	207 ± 16	222	222	218 ± 22	222 ± 49
PCho R	127	102	189	190	250 ± 4	205 ± 11	-	-	-	-	178 ± 20	191 ± 49

published version at https://doi.org/10.1002/nbm.4328

List of Abbreviations

2DJ-IR – Two Dimensional J-resolved Inversion Recovery
Asp – Aspartate
Cr – Creatine
CRLB – Cramér Rao Lower Bounds
CSF – Cerebrospinal fluid
GABA – γ-aminobutyric-acid
Glc – Glucose
Gln – Glutamine
Glu – Glutamate
Gly – Glycine
GM – Grey Matter
GPC – Glycerophosphorylcholine
GSH – Glutathione
Lac – Lactate
MEM – Mono-Exponential decay Model
mI – myo-Inositol
MM - Macromolecular
MMBG – Macromolecular Background
NAA – N-acetylaspartate
NAAG – N-acetylaspartylglutamate
PCho – Phosphocholine
PCr – Phosphocreatine
PE – Phosphorylethanolamine
sI – scyllo-Inositol
Tau – Taurine
TE – Echo Time
TI – Inversion Time
VOI – Volume Of Interest
WM – White Matter

published version at https://doi.org/10.1002/nbm.4328

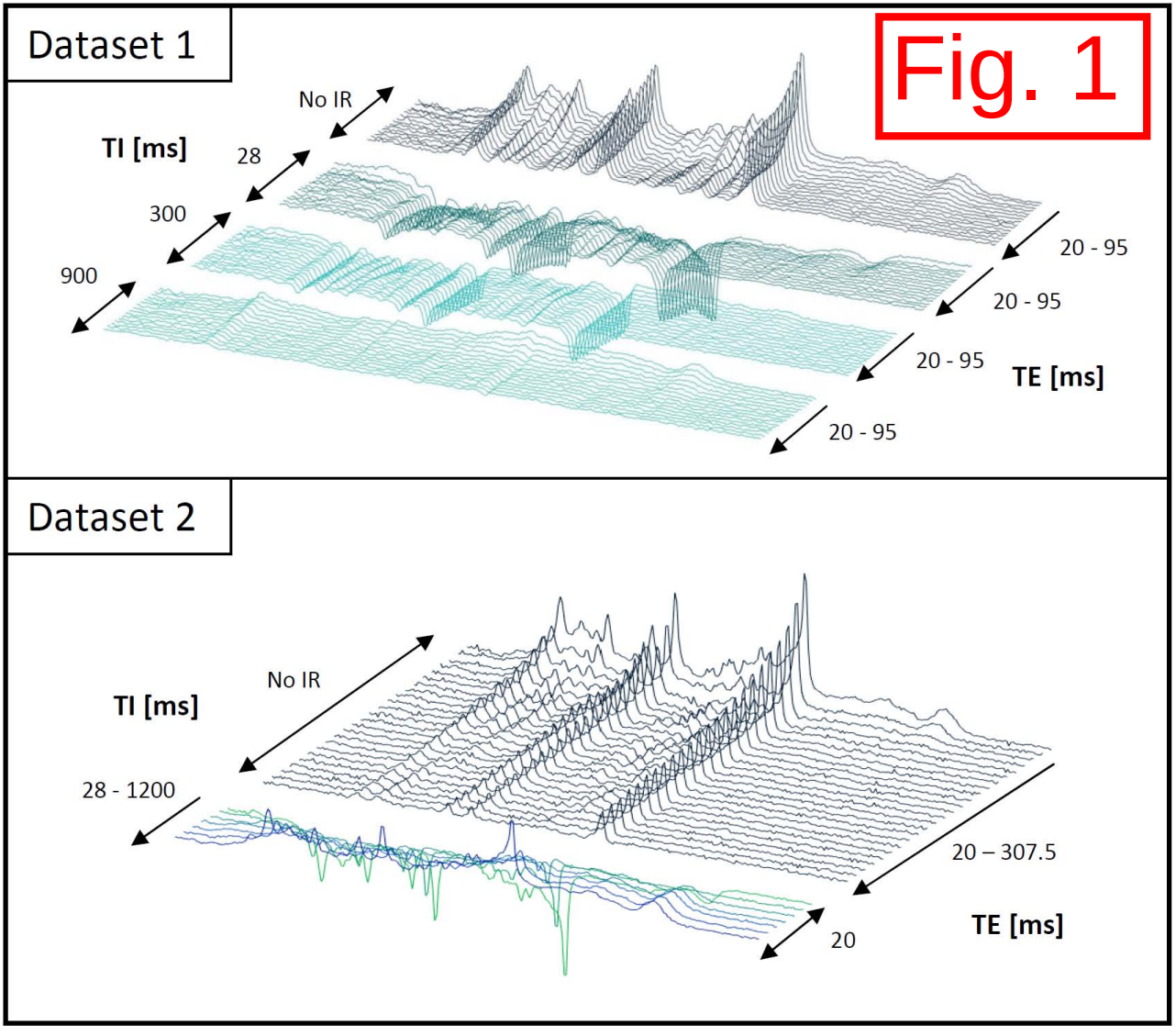
Dataset 1
Fig. 1
TI [ms]
No IR
28
300
900
20 - 95
20 - 95
20 - 95
20 - 95
TE [ms]
Dataset 2
TI [ms]
No IR
28 - 1200
20 – 307.5
20
TE [ms]

Three different modeling methods for the MMBG

Fig. 2

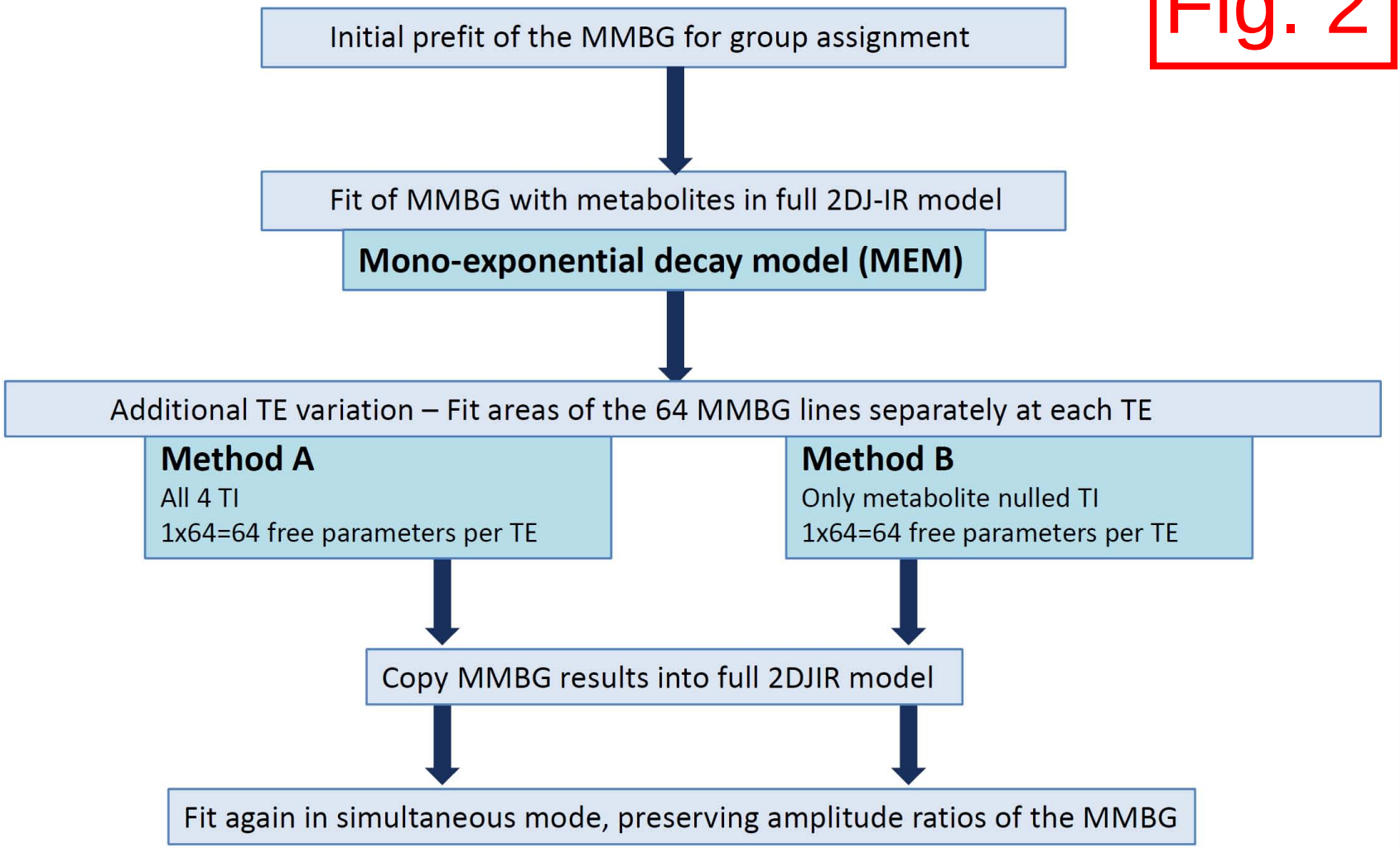

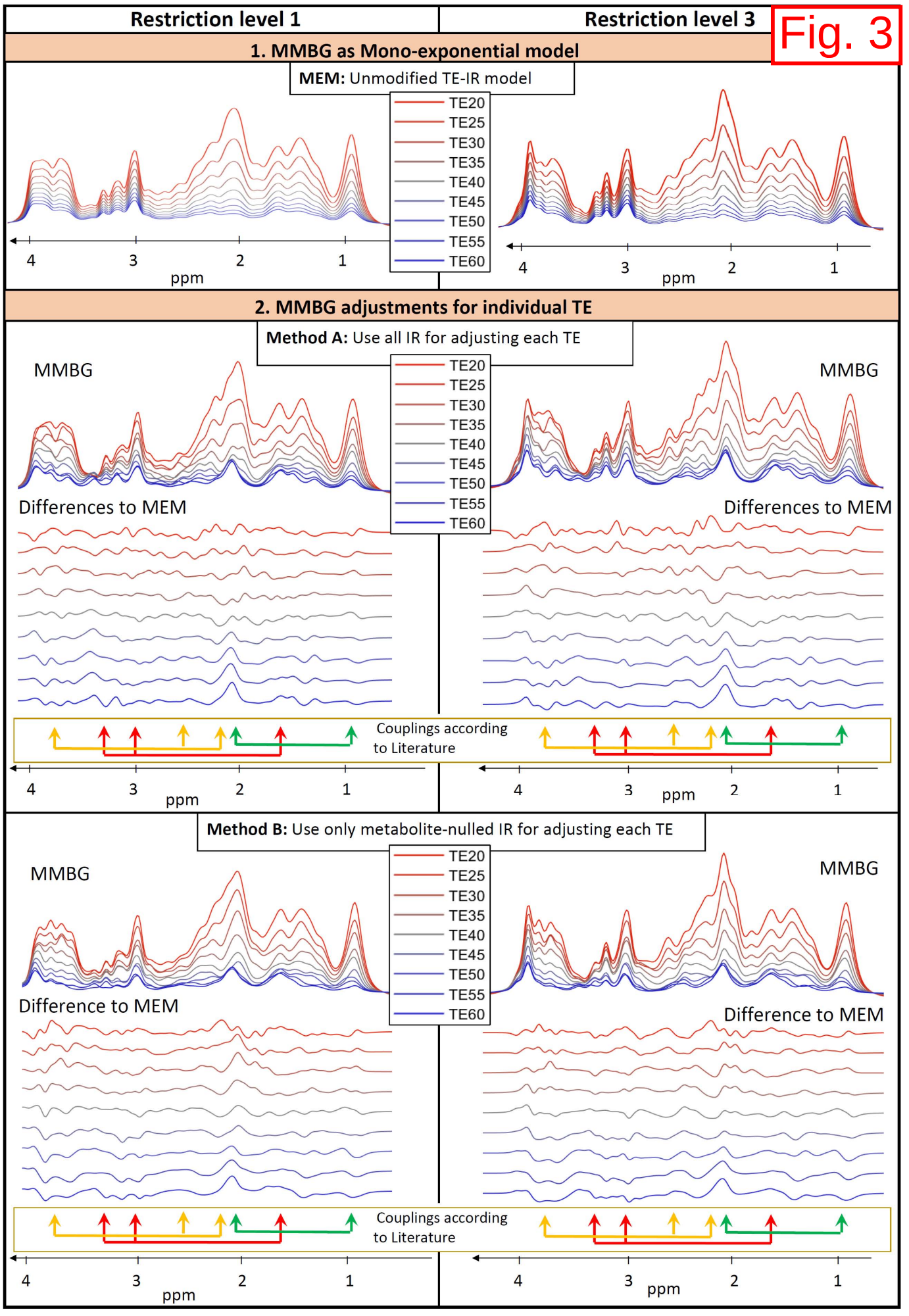
Restriction level 1
Restriction level 3
Fig. 3
1. MMBG as Mono-exponential model
MEM: Unmodified TE-IR model
TE20
TE25
TE30
TE35
TE40
TE45
TE50
TE55
TE60
4
3
2
1
ppm
2. MMBG adjustments for individual TE
Method A: Use all IR for adjusting each TE
MMBG
Differences to MEM
Couplings according to Literature
Method B: Use only metabolite-nulled IR for adjusting each TE
Difference to MEM

Influence of MMBG model on metabolite evaluation – Restriction Level 3

Fig. 4

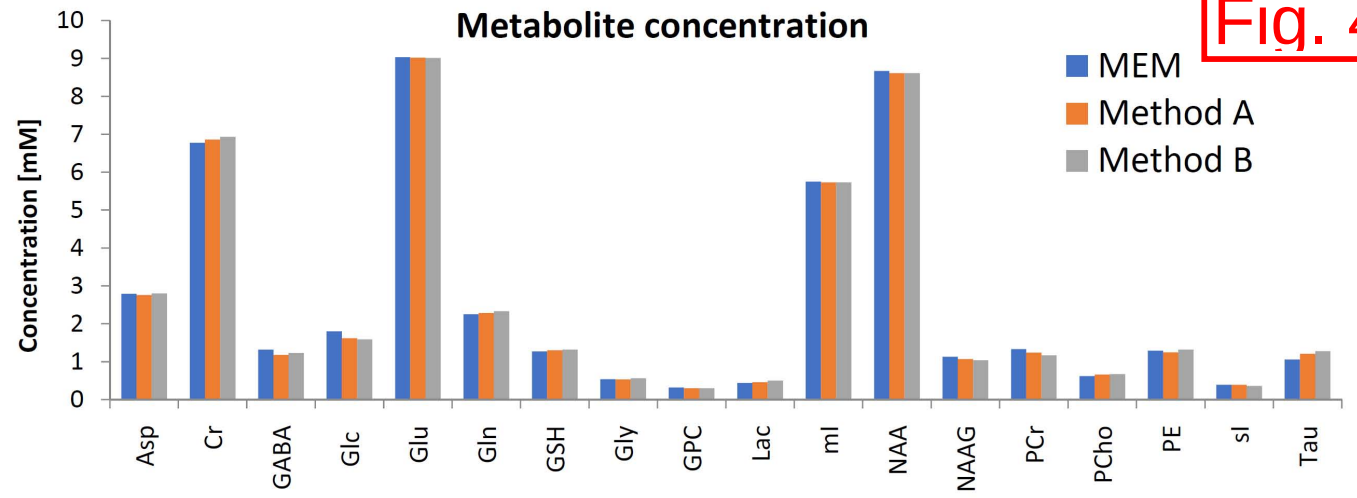

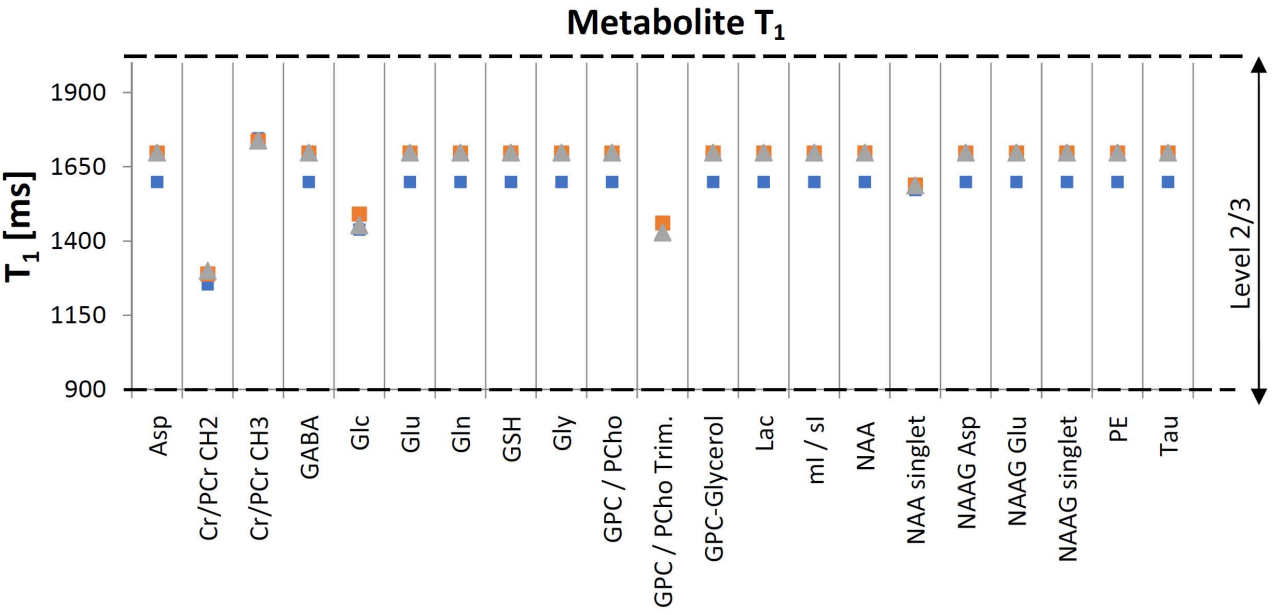

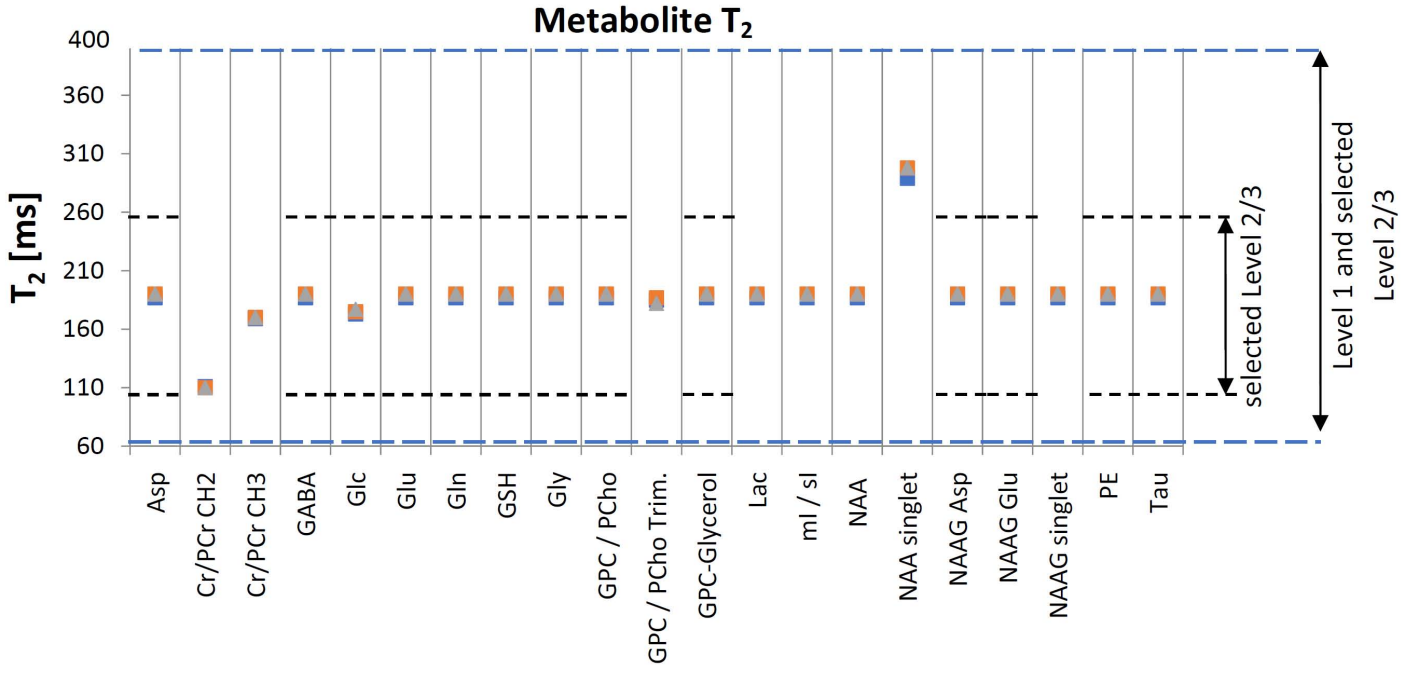

Influence of restriction level on metabolite evaluation

Fig. 5

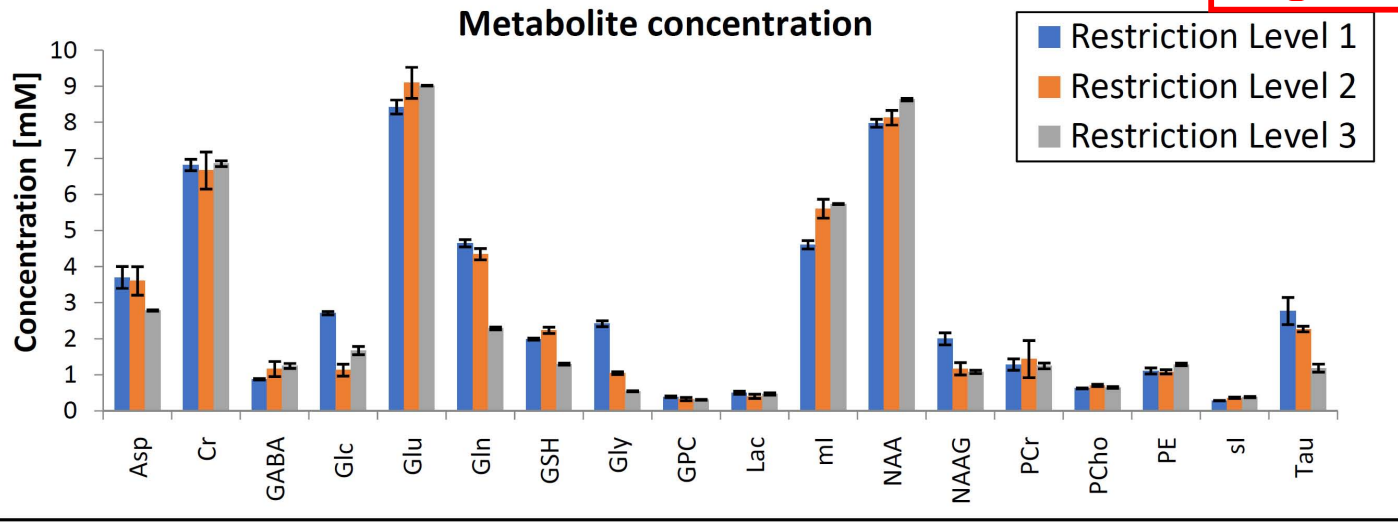

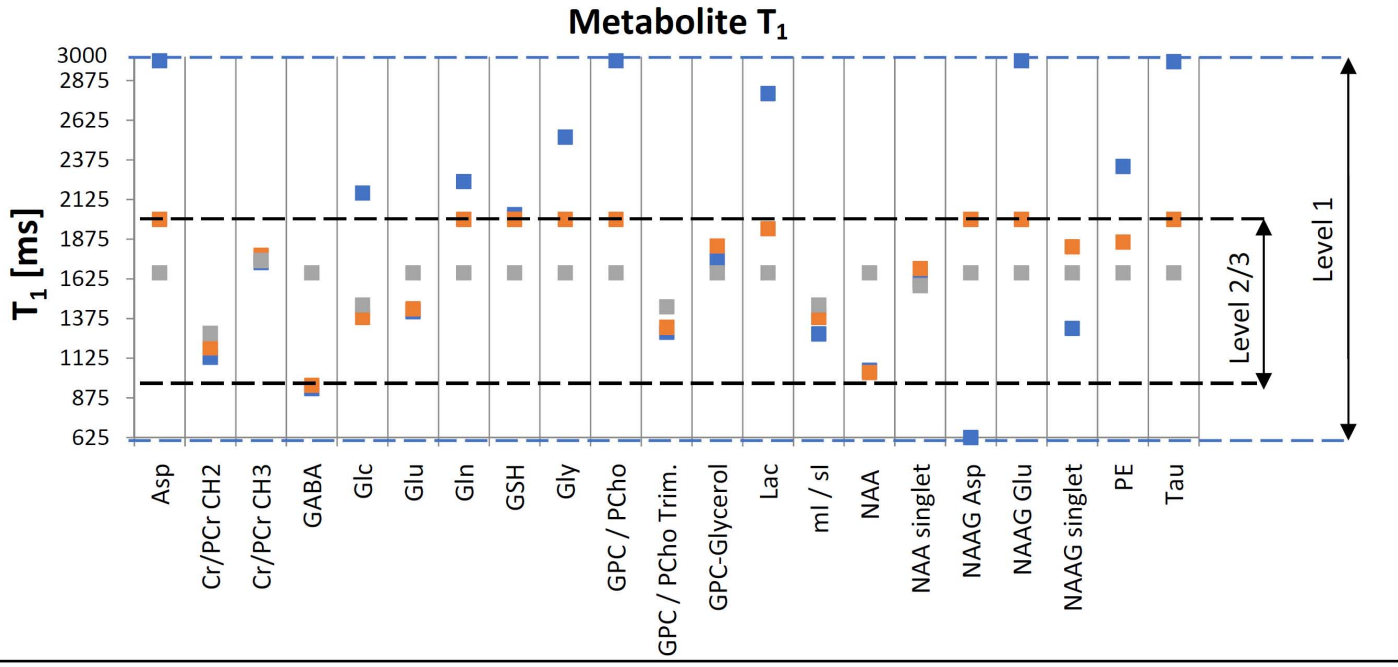

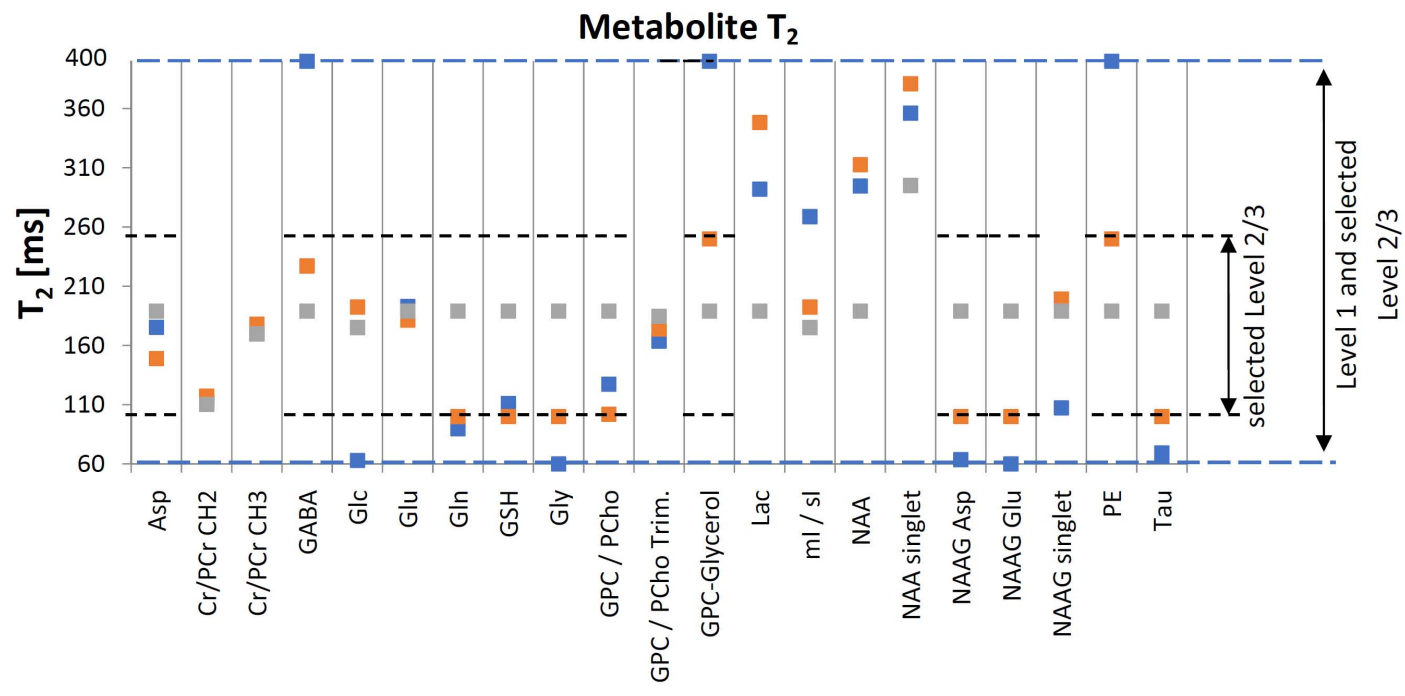

Fig. 6

Restriction level 1

No IR

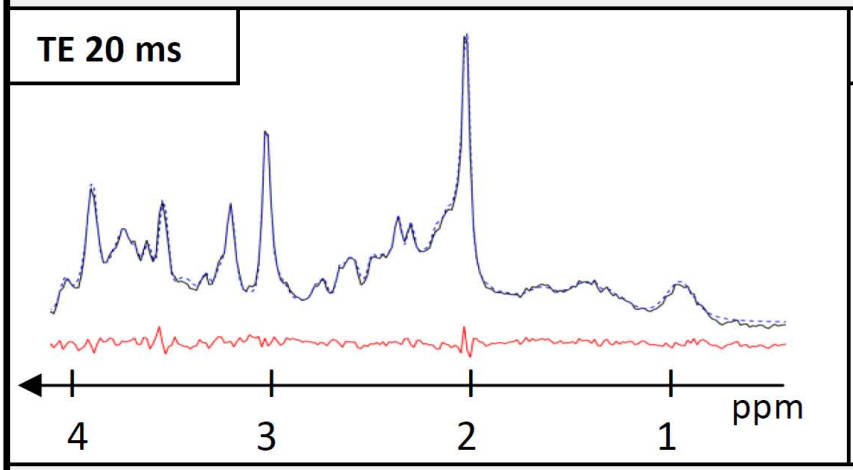

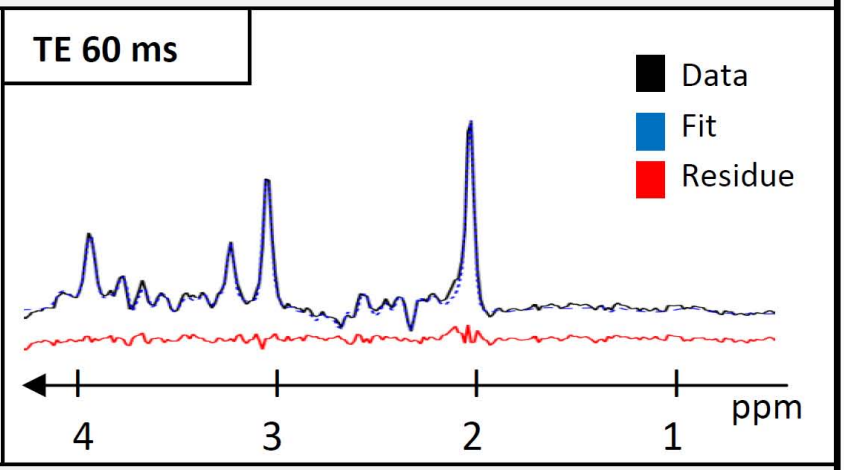

Metabolite nulled TI=900 ms

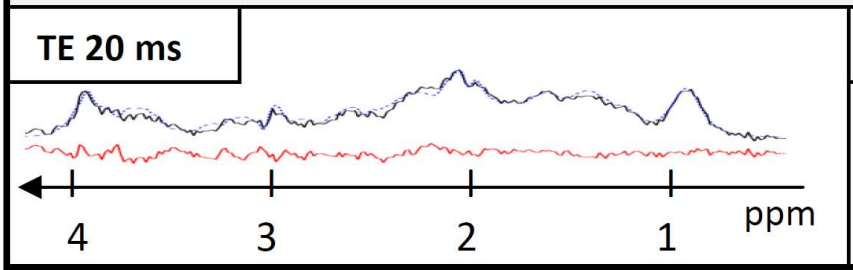

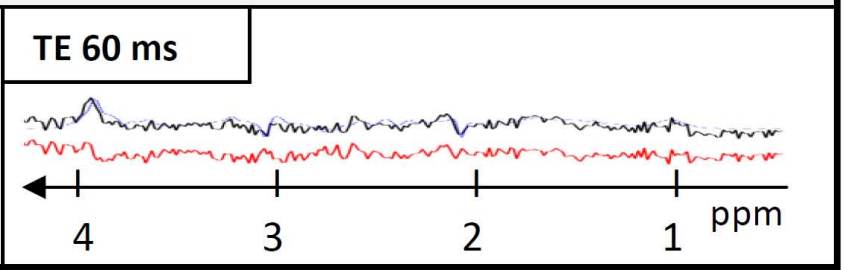

Restriction level 3

No IR

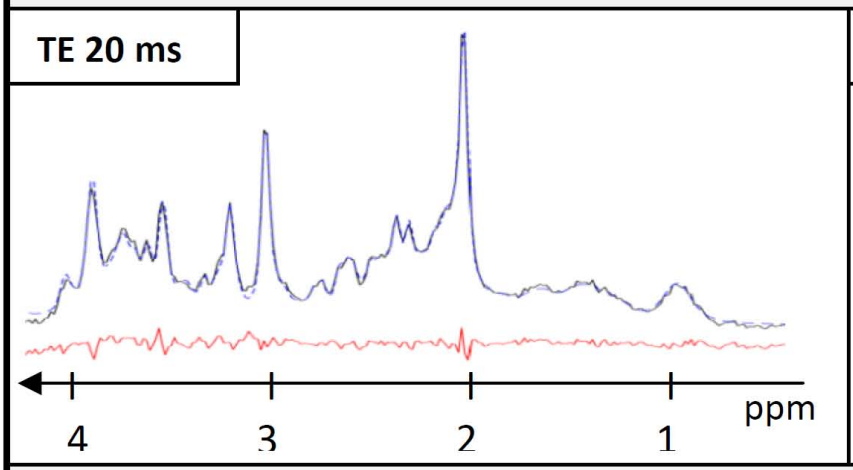

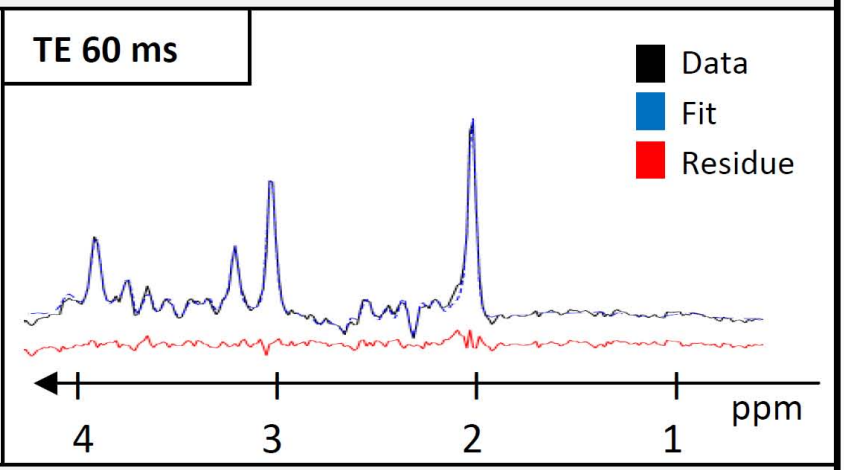

Metabolite nulled TI=900 ms

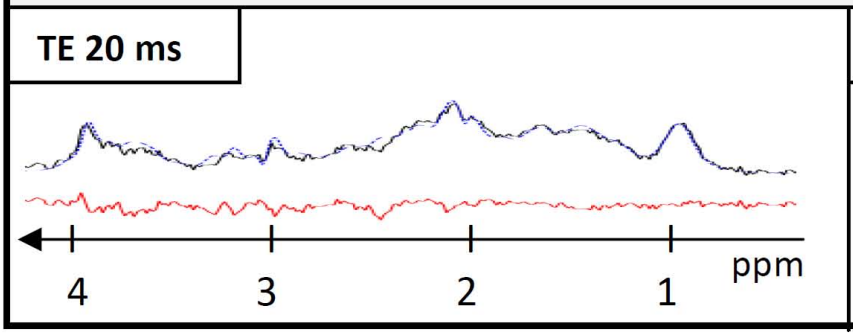

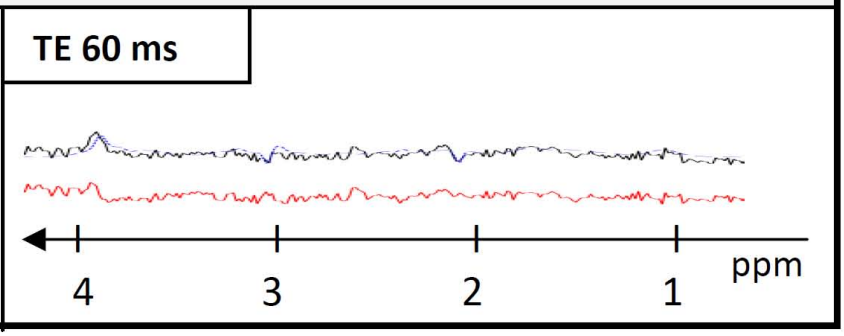

Fig. 7

Metabolite concentrations in WM and GM

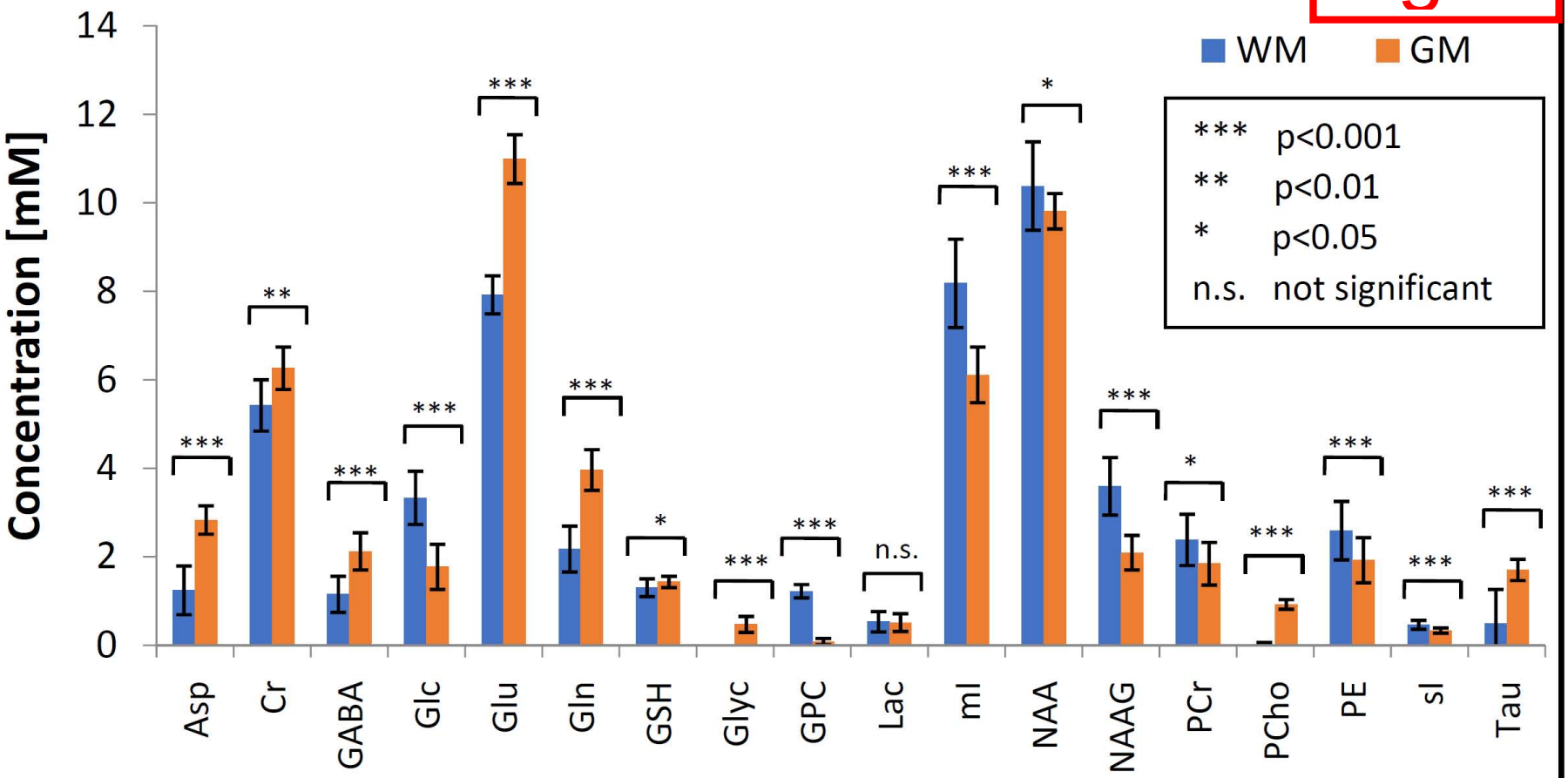

Metabolite relaxation times in WM and GM

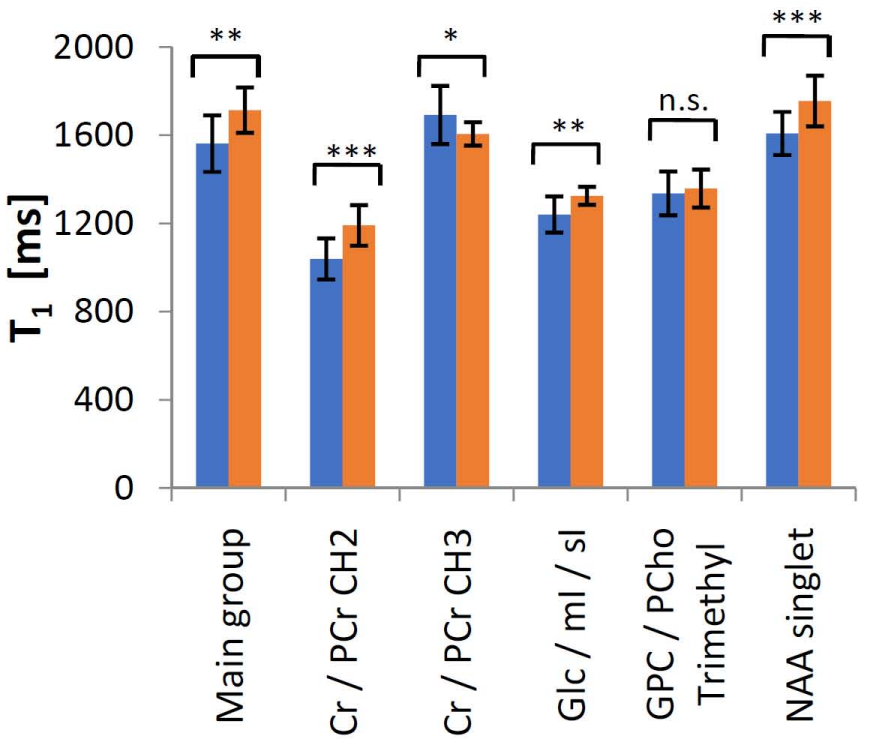

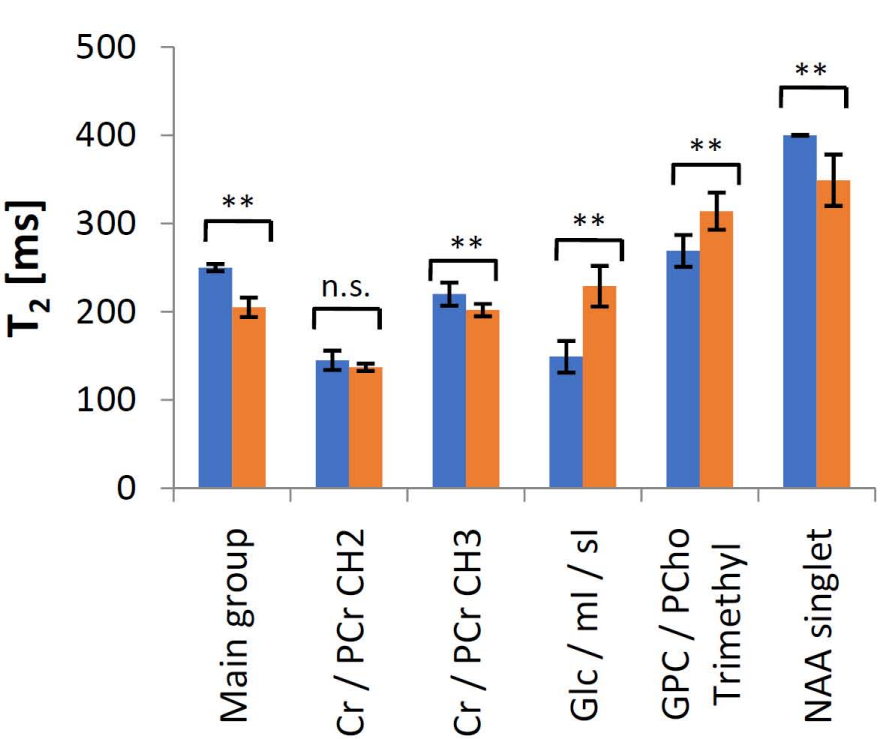

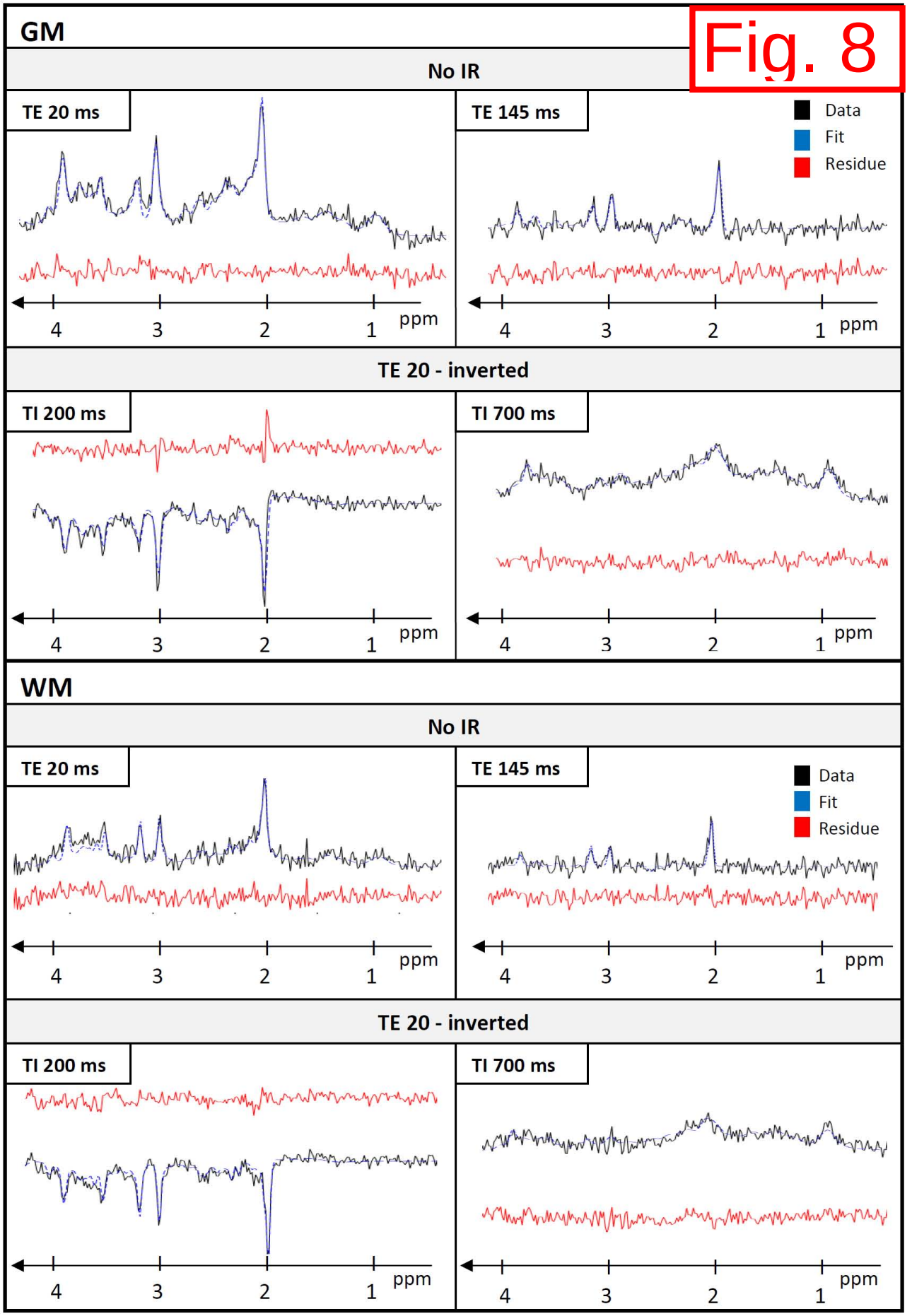
Fig. 8
GM
No IR
TE 20 ms
TE 145 ms
Data
Fit
Residue
4
3
2
1
ppm
TE 20 - inverted
TI 200 ms
TI 700 ms
WM
No IR
TE 20 ms
TE 145 ms
Data
Fit
Residue
TE 20 - inverted
TI 200 ms
TI 700 ms

Stability of concentration evaluation

Fig. 9

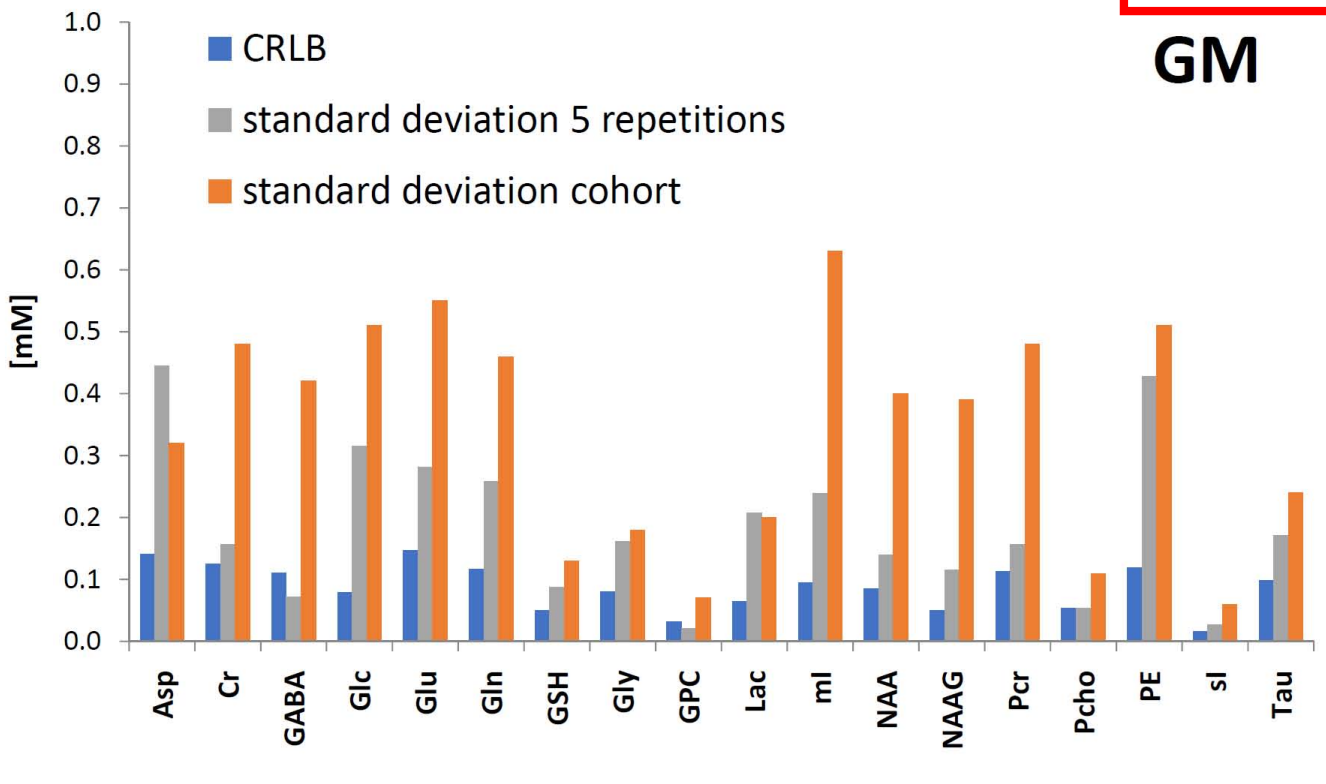

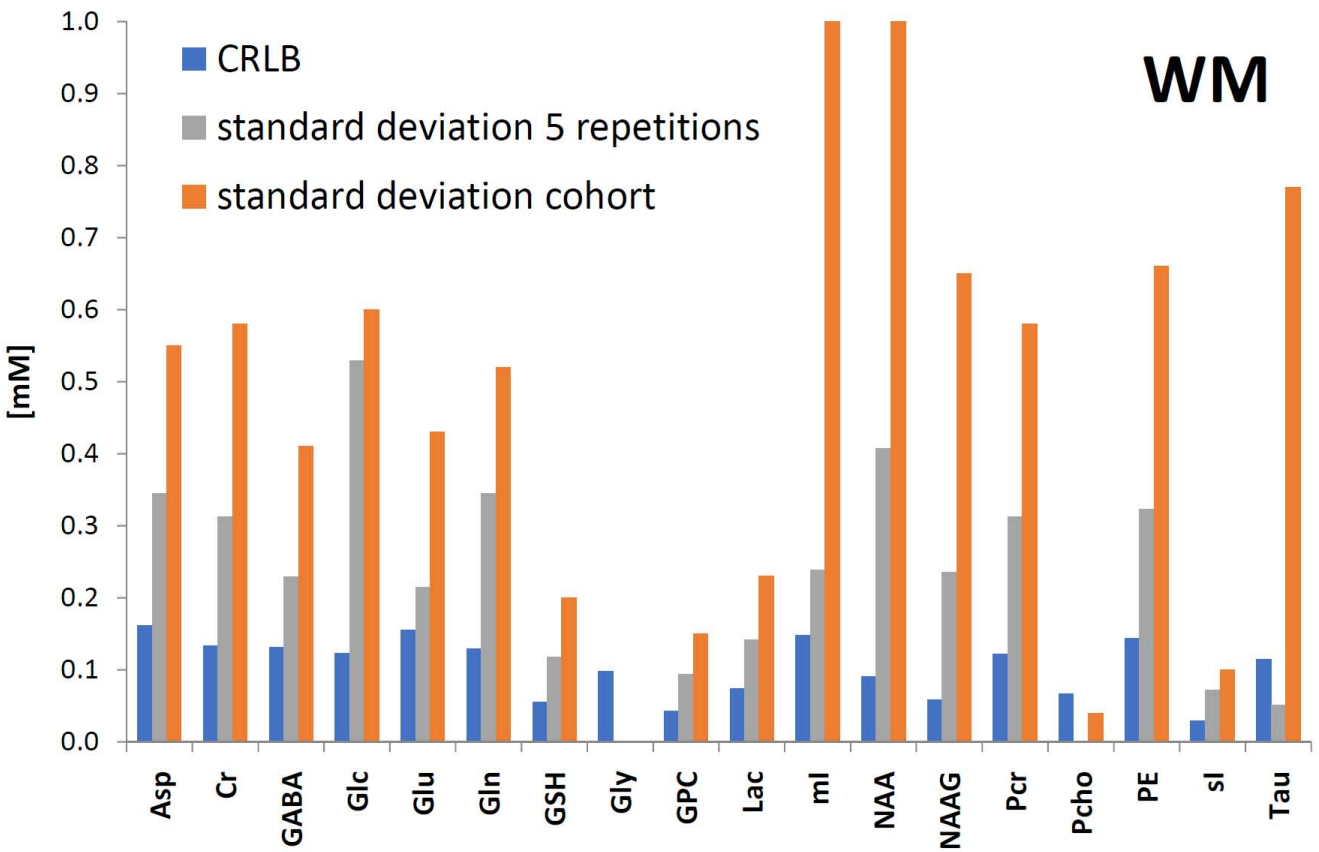

Supplements

S1. Voxel Placement

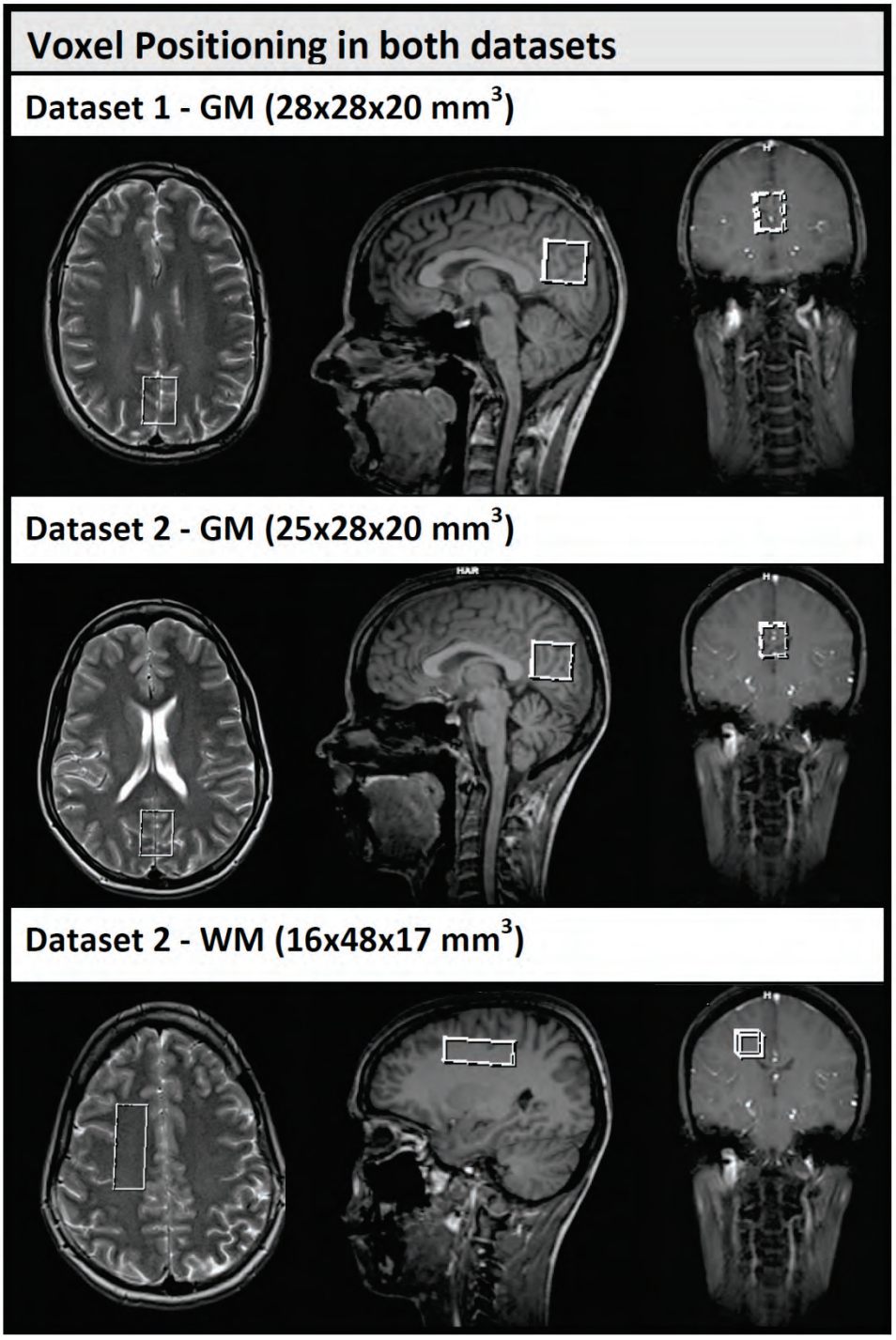

Figure S1 – *Illustration of voxel placement in both dataset 1 and dataset 2 measurements.*

S2. Pre-Fit for grouping of constituent resonance lines of the MMBG into parts with equal relaxation times

To allow some, but not total variation of T_1 and T_2 between different parts of the MM included in the MMBG, a grouping of the equally spaced lines was performed. To get a first impression of the expected shape of the MMBG, a pre-fit on the not inverted spectra at the TE range between 20 and 60 ms was applied. All metabolite parameters (except T_1) and the area of the MMBG lines were fitted, while the T_1 and T_2 of the MMBG were held constant at 250 ms and 20 ms, respectively. Next, the MMBG was separated at its minimum intensity values, allowing a maximum number of 8 lines in one group, resulting in 11 MM resonance groups. This partitioning was retained for all following models and each group was assigned an individual T_1 and T_2 parameter, which was then allowed to adapt individually.

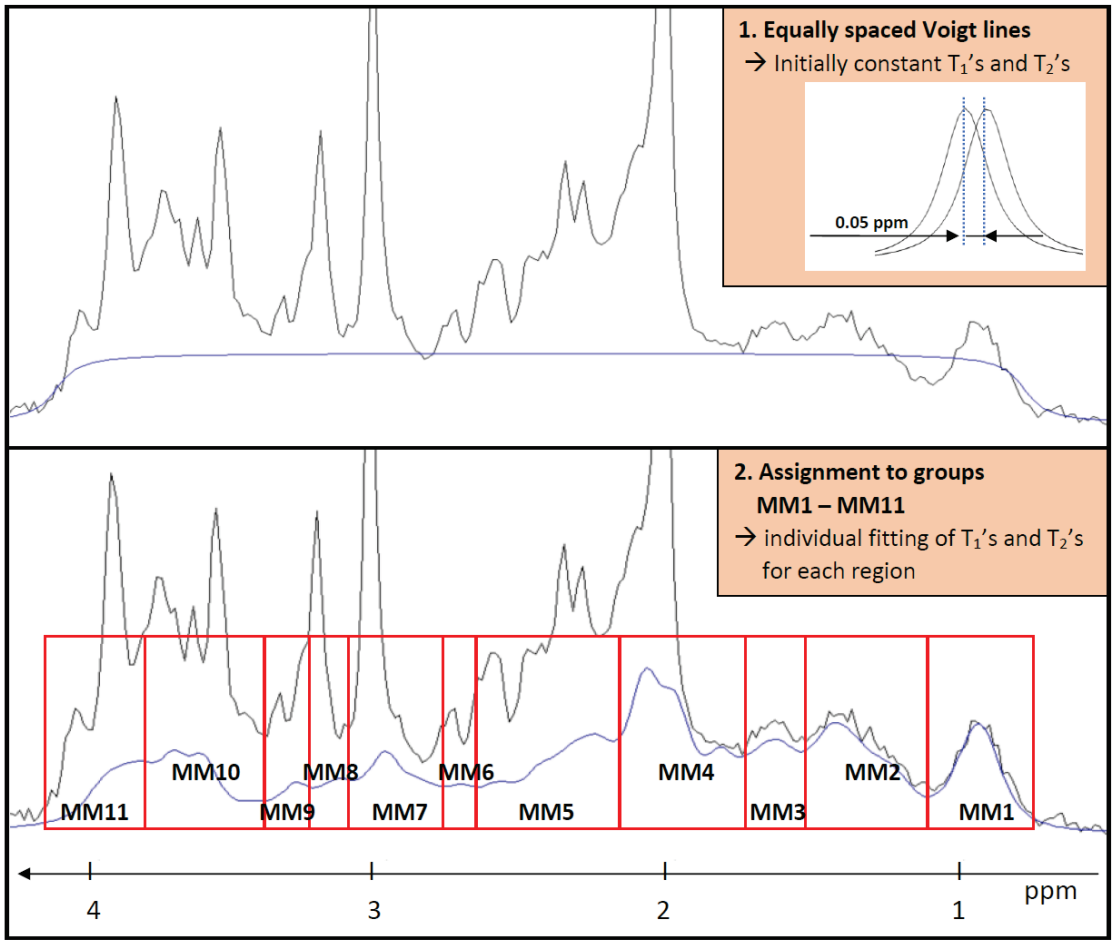

Figure S2 – *Illustration of MMBG modeling: Above: Equally and closely spaced Voigt lines with fixed Lorentzian and Gaussian broadening were fitted to the MMBG (initial state before fitting with equal amplitudes of all Voigt lines). Below: First fitting result for a TE of 20 ms and no IR; MMBG was grouped into 11 partitions at minimum values to allow subsequent T_1 and T_2 variation. Beware, the MM group labeling is not according to convention, but rather represents a consecutive numbering resulting from the prefit step mentioned.*

S3. T_1 and T_2 relaxation times for the MM groups in all fitting models

T_1 [ms]	Restriction level 1			Restriction level 2			Restriction level 3		
MMBL Model	MEM	A	B	MEM	A	B	MEM	A	B
MM1	289	288	287	288	288	287	291	290	289
MM2	308	306	300	316	314	307	311	309	305
MM3	234	227	227	217	217	220	231	225	230
MM4	209	222	235	254	267	280	231	247	248
MM5	243	227	244	206	205	223	263	263	258
MM6	399	376	335	400	383	305	400	400	400
MM7	400	400	400	400	400	400	400	400	400
MM8	400	400	400	400	400	400	400	400	400
MM9	400	400	400	400	400	400	400	400	400
MM10	400	400	400	400	400	400	400	400	400
MM11	318	327	310	348	340	326	338	347	340

T_2 [ms]	Restriction level 1			Restriction level 2			Restriction level 3		
MMBL Model	MEM	A	B	MEM	A	B	MEM	A	B
MM1	20	21	21	21	21	22	20	21	21
MM2	20	19	22	21	20	23	20	19	22
MM3	25	26	24	20	23	20	25	27	24
MM4	16	22	23	22	25	30	17	19	21
MM5	22	23	21	19	21	20	20	24	20
MM6	19	18	19	18	17	18	16	16	16
MM7	35	35	35	35	35	35	35	35	35
MM8	35	35	35	35	35	35	35	35	35
MM9	35	35	35	35	35	35	35	35	32
MM10	24	23	24	24	23	25	24	24	25
MM11	35	34	35	35	35	35	35	34	34

Table S3 – *T_1 and T_2 relaxation times for the MM groups in all fitting models (dataset 1). Variations between the MMBG models and restriction levels are commonly small. MM groups towards higher ppm values mostly reach the upper border for both T_1 and T_2.*

S4. MMBG Models at TE 20 ms for MEM and Method A in Restriction Level 3

MMBG Amplitudes for TE 20 ms and Restriction Level 3			MEM	Method A
Line	**MM Group**	**Frequency offset [ppm]**	**Amplitude**	**Amplitude**
Line 1	MM1	0.784	0.0000	0.0000
Line 2	MM1	0.837	0.0000	0.0000
Line 3	MM1	0.890	32.4953	42.7346
Line 4	MM1	0.942	109.6302	87.9366
Line 5	MM1	0.995	48.0284	54.9499
Line 6	MM1	1.048	5.4860	0.9890
Line 7	MM2	1.101	0.0000	0.0000
Line 8	MM2	1.153	0.0000	0.4817
Line 9	MM2	1.206	18.2067	14.2943
Line 10	MM2	1.259	45.1294	52.0078
Line 11	MM2	1.312	18.9602	13.4369
Line 12	MM2	1.364	42.4103	37.3393
Line 13	MM2	1.417	54.3822	73.2872
Line 14	MM2	1.470	64.3125	61.9803
Line 15	MM3	1.523	19.7283	18.2343
Line 16	MM3	1.575	15.6043	11.9116
Line 17	MM3	1.628	39.2875	39.5380
Line 18	MM3	1.681	33.4707	29.7157
Line 19	MM3	1.734	23.8722	29.3843
Line 20	MM3	1.786	0.0000	1.5585
Line 21	MM4	1.839	80.3948	68.3158
Line 22	MM4	1.892	0.0000	0.0000
Line 23	MM4	1.945	0.0000	0.0000
Line 24	MM4	1.998	137.4897	132.5962
Line 25	MM4	2.050	0.0000	0.0000
Line 26	MM4	2.103	249.8545	183.2250
Line 27	MM4	2.156	23.1049	38.0108
Line 28	MM5	2.209	0.0000	16.0862
Line 29	MM5	2.261	63.7799	64.9917
Line 30	MM5	2.314	36.6025	5.6337
Line 31	MM5	2.367	43.5821	63.5133
Line 32	MM5	2.420	15.0980	2.4240
Line 33	MM5	2.472	57.9974	35.2566
Line 34	MM5	2.525	5.8520	14.3901
Line 35	MM5	2.578	12.7799	0.5754
Line 36	MM5	2.631	47.4578	45.3905
Line 37	MM6	2.683	18.3663	0.9906
Line 38	MM6	2.736	0.0000	29.0325
Line 39	MM6	2.789	28.2640	39.3170
Line 40	MM6	2.842	38.3264	3.4445

Line 41	MM7	2.894	9.0032	13.0130
Line 42	MM7	2.947	0.0000	0.1879
Line 43	MM7	3.000	38.2491	42.7107
Line 44	MM7	3.053	24.5820	15.6513
Line 45	MM8	3.105	5.4876	16.2569
Line 46	MM8	3.158	0.0000	0.0000
Line 47	MM8	3.211	32.4535	28.2194
Line 48	MM8	3.264	0.0000	2.3004
Line 49	MM9	3.316	18.4564	16.2628
Line 50	MM9	3.369	0.0000	0.4789
Line 51	MM9	3.422	0.0000	0.0000
Line 52	MM10	3.475	11.9632	3.4288
Line 53	MM10	3.528	0.0000	10.7709
Line 54	MM10	3.580	11.0819	1.0635
Line 55	MM10	3.633	33.4769	44.5833
Line 56	MM10	3.686	30.1254	14.6264
Line 57	MM10	3.739	42.7429	46.1329
Line 58	MM10	3.791	19.6077	29.4814
Line 59	MM11	3.844	21.6605	23.3754
Line 60	MM11	3.897	11.6076	13.1324
Line 61	MM11	3.905	50.0351	48.5184
Line 62	MM11	4.002	0.0000	0.0000
Line 63	MM11	4.055	7.7713	2.1130
Line 64	MM11	4.108	0.0000	0.0000

Table S4 – *Amplitudes for the 64 Voigt Lines of the MMBG Model for TE 20 ms, Restriction Level 3, MEM and Method A. Related relaxation times for each MM group are listed in Table S3; Gaussian broadening was 5 Hz and the phase was identical for all components.*

S5. Table of estimated metabolite concentrations for dataset 1 for all restriction levels and all MMBG models

Concentration [mM]	Restriction level 1			Restriction level 2			Restriction level 3		
MMBL Model	MEM	A	B	MEM	A	B	MEM	A	B
Asp	3.43	3.64	4.03	3.31	3.45	4.05	2.79	2.76	2.8
Cr	6.64	6.87	6.94	6.07	6.92	7.00	6.77	6.86	6.93
GABA	0.9	0.86	0.87	1.40	1.01	1.07	1.32	1.18	1.23
Glc	2.76	2.67	2.70	1.32	1.05	1.02	1.80	1.62	1.59
Glu	8.59	8.47	8.21	9.51	9.12	8.65	9.03	9.02	9.01
Gln	4.55	4.75	4.64	4.49	4.36	4.18	2.25	2.28	2.33
GSH	2.02	1.97	1.97	2.33	2.21	2.16	1.27	1.30	1.32
Gly	2.43	2.49	2.33	1.09	1.04	1.01	0.54	0.53	0.56
GPC	0.41	0.37	0.39	0.38	0.30	0.30	0.32	0.30	0.30
Lac	0.47	0.49	0.55	0.38	0.36	0.47	0.44	0.46	0.5
mI	4.74	4.54	4.54	5.91	5.44	5.47	5.75	5.73	5.73
NAA	8.06	8.01	7.85	8.36	8.01	8.01	8.67	8.61	8.61
NAAG	2.17	1.98	1.84	1.35	1.13	1.02	1.13	1.07	1.04
PCr	1.46	1.23	1.16	2.03	1.18	1.1	1.33	1.24	1.17
PCho	0.61	0.64	0.62	0.67	0.72	0.73	0.62	0.66	0.67
PE	1.2	1.06	1.06	1.15	1.04	1.06	1.29	1.25	1.32
sI	0.29	0.28	0.28	0.38	0.35	0.35	0.39	0.39	0.36
Tau	2.53	3.20	2.57	2.18	2.30	2.32	1.06	1.21	1.28

Table S5 – *Estimated concentrations for all metabolites included in the model for all three levels of restriction and the three modeling methods for the MMBG (dataset 1). Variations between the MMBG models are commonly small, while variations between the restriction levels are significant for some metabolites.*

S6. Table of T_1 relaxation times for all restriction levels and all MMBG models

T_1 [ms]		Restriction level 1			Restriction level 2			Restriction level 3		
MMBL model		MEM	A	B	MEM	A	B	MEM	A	B
Asp		3000	3000	3000	2000	2000	2000	1599	1696	1698
Cr	CH_2	1120	1129	1145	1174	1189	1210	1254	1289	1300
	CH_3	1747	1721	1716	1825	1744	1755	1746	1737	1738
GABA		944	997	864	952	1016	900	Asp	Asp	Asp
Glc		1537	2232	2730	1332	1409	1407	1439	1491	1453
Glu		1378	1395	1484	1372	1381	1559	Asp	Asp	Asp
Gln		2222	1734	2761	2000	2000	2000	Asp	Asp	Asp
GSH		2008	2110	1974	2000	2000	2000	Asp	Asp	Asp
Gly		2481	2516	2557	2000	2000	2000	Asp	Asp	Asp
GPC	Cho	3000	3000	3000	2000	2000	2000	Asp	Asp	Asp
	Cho-Trimethyl	1290	1295	1282	1324	1330	1306	1460	1461	1429
	Glycerol	1842	1823	1553	1989	1820	1690	Asp	Asp	Asp
Lac		3000	3000	2377	2000	2000	1823	Asp	Asp	Asp
mI		1245	1280	1309	Glc	Glc	Glc	Glc	Glc	Glc
NAA	R	1065	1035	1051	1052	1016	1039	Asp	Asp	Asp
	Singlet	1591	1596	1631	1700	1689	1686	1572	1589	1587
NAAG	Asp	625	625	625	GSH	GSH	GSH	Asp	Asp	Asp
	Glu	3000	3000	3000	GSH	GSH	GSH	Asp	Asp	Asp
	Singlet	1191	1315	1437	1670	1821	1994	Asp	Asp	Asp
PCr	CH_2	Cr H_2	Cr H_2	Cr H_2	Cr H_2	Cr H_2	Cr H_2	Cr H_2	Cr H_2	Cr H_2
	CH_3	Cr H_3	Cr H_3	Cr H_3	Cr H_3	Cr H_3	Cr H_3	Cr H_3	Cr H_3	Cr H_3
PCho	Trimethyl	GPC Cho-Tri.	GPC Cho-Tri.	GPC Cho-Tri.	GPC Cho-Tri.	GPC Cho-Tri.	GPC Cho-Tri.	GPC Cho-Tri.	GPC Cho-Tri.	GPC Cho-Tri.
	R	GPC Cho	GPC Cho	GPC Cho	GPC Cho	GPC Cho	GPC Cho	Asp	Asp	Asp
PE		2897	2523	1579	2000	2000	1573	Asp	Asp	Asp
sI		mI	mI	mI	Glc	Glc	Glc	Glc	Glc	Glc
Tau		3000	2979	3000	2000	2000	2000	Asp	Asp	Asp

Table S6 - *Results for T_1 relaxation data for all three levels of restriction and modeling methods for the MMBG (dataset 1). Parameters reaching the predefined borders are displayed in grey; linked parameters are marked by corresponding metabolite. Variations between the MMBG models are noticeable for several metabolites. For the different restriction levels, variations are detectable for all metabolites, not only the ones with a modified restriction range.*

S7. Table of T_2 relaxation times for all restriction levels and all MMBG models

T_2 [ms]		Restriction level 1			Restriction level 2			Restriction level 3		
MMBL model		MEM	A	B	MEM	A	B	MEM	A	B
Asp		196	177	153	178	146	123	187	190	190
Cr	CH_2	115	113	111	124	115	113	111	110	110
	CH_3	172	170	168	191	173	170	169	170	170
GABA		400	400	400	181	250	250	Asp	Asp	Asp
Glc		64	60	65	188	197	192	173	175	177
Glu		189	191	199	178	175	191	Asp	Asp	Asp
Gln		90	82	97	100	100	100	Asp	Asp	Asp
GSH		109	114	110	100	100	100	Asp	Asp	Asp
Gly		60	60	60	100	100	100	Asp	Asp	Asp
GPC	Cho	110	121	151	100	100	106	Asp	Asp	Asp
	Cho-Trimethyl	163	166	162	175	176	171	185	187	182
	Glycerol	400	400	400	250	250	250	Asp	Asp	Asp
Lac		348	313	215	400	400	245	Asp	Asp	Asp
mI		256	275	275	Glc	Glc	Glc	Glc	Glc	Glc
NAA	R	291	290	303	321	312	305	Asp	Asp	Asp
	Singlet	353	349	366	400	377	366	289	298	298
NAAG	Asp	60	71	60	GSH	GSH	GSH	Asp	Asp	Asp
	Glu	60	60	60	GSH	GSH	GSH	Asp	Asp	Asp
	Singlet	103	105	114	187	198	213	Asp	Asp	Asp
PCr	CH_2	Cr H_2	Cr H_2	Cr H_2	Cr H_2	Cr H_2	Cr H_2	Cr H_2	Cr H_2	Cr H_2
	CH_3	Cr H_3	Cr H_3	Cr H_3	Cr H_3	Cr H_3	Cr H_3	Cr H_3	Cr H_3	Cr H_3
PCh	Trimethyl	GPC Cho-Tri.	GPC Cho-Tri.	GPC Cho-Tri.	GPC Cho-Tri.	GPC Cho-Tri.	GPC Cho-Tri.	GPC Cho-Tri.	GPC Cho-Tri.	GPC Cho-Tri.
	R	GPC Cho	GPC Cho	GPC Cho	GPC Cho	GPC Cho	GPC Cho	GPC Cho	GPC Cho	GPC Cho
PE		400	400	400	250	250	250	Asp	Asp	Asp
sI		mI	mI	mI	Glc	Glc	Glc	Glc	Glc	Glc
Tau		69	60	79	100	100	100	Asp	Asp	Asp

Table S7 - *Results for T_2 relaxation for all three levels of restriction and modeling methods for the MMBG (dataset 1). Parameters reaching the predefined borders are displayed in grey; linked parameters are marked with corresponding metabolite. As for T_1, variations between the MMBG models are noticeable for several metabolites. For the different restriction levels, variations are detectable for all metabolites, not only the ones with a modified restriction range.*

S8. Table of metabolite concentrations for dataset 2: GM and WM VOIs

Concentration [mM]	Fitting sum spectra from all subjects		Fitting individual subjects data		
	WM	GM	WM	GM	p
Asp	1.25	2.85	1.24 ± 0.55	2.83 ± 0.32	< 0.001
Cr	5.31	6.31	5.42 ± 0.58	6.26 ± 0.48	0.002
GABA	1.17	2.19	1.15 ± 0.41	2.12 ± 0.42	< 0.001
Glc	3.36	1.83	3.33 ± 0.60	1.77 ± 0.51	< 0.001
Glu	7.94	11.00	7.92 ± 0.43	10.99 ± 0.55	< 0.001
Gln	2.21	3.97	2.17 ± 0.52	3.96 ± 0.46	< 0.001
GSH	1.32	1.42	1.30 ± 0.20	1.43 ± 0.13	0.03
Glyc	0.00	0.48	0.00 ± 0.00	0.47 ± 0.18	< 0.001
GPC	1.24	0.10	1.22 ± 0.15	0.08 ± 0.07	< 0.001
Lac	0.54	0.50	0.53 ± 0.23	0.51 ± 0.20	>0.05
mI	8.19	6.13	8.18 ± 1.00	6.11 ± 0.63	< 0.001
NAA	10.37	9.80	10.38 ± 1.00	9.81 ± 0.40	0.03
NAAG	3.67	2.08	3.59 ± 0.65	2.09 ± 0.39	< 0.001
PCr	2.49	1.79	2.38 ± 0.58	1.84 ± 0.48	0.02
PCho	0.00	0.89	0.02 ± 0.04	0.92 ± 0.11	< 0.001
PE	2.65	2.01	2.59 ± 0.66	1.92 ± 0.51	< 0.001
sI	0.46	0.33	0.46 ± 0.10	0.33 ± 0.06	< 0.001
Tau	0.29	1.62	0.49 ± 0.77	1.70 ± 0.24	< 0.001

Table S8 – *Results for metabolite concentration estimates in dataset 2 for fitting individual subjects and also the sum spectra over all subjects, which are in good agreement. P-values, obtained by a paired t-test, indicate significant differences between GM and WM content for all metabolites except Lac.*

S9. Table of estimated metabolite relaxation time T_1 for dataset 2: GM and WM

T1 [ms]	Fitting sum spectra from all subjects		Fitting individual subjects		
	WM	GM	WM	GM	p
Asp, GABA, Glu, Gln, GSH, Gly, GPC, Lac, NAA R, NAAG, PE, Tau	1560	1691	1562 ± 128	1714 ± 103	0.002
Cr / PCr CH_2	1028	1171	1039 ± 93	1191 ± 92	< 0.001
Cr / PCr CH_3	1671	1598	1692 ± 132	1606 ± 53	0.03
Glc, mI, sI	1236	1322	1240 ± 82	1325 ± 41	0.002
GPC / PCho Trimethyl	1325	1349	1336 ± 100	1358 ± 86	>0.05
NAA singlet	1608	1735	1608 ± 98	1755 ± 115	< 0.001

Table S9 – *Results for metabolite relaxation time T_1 in dataset 2 for fitting individual subjects and also the sum spectra over all subjects, which are in good agreement. P-values, obtained by a paired t-test, indicate significant differences between GM and WM content for all metabolites except the GPC/PCho trimethyl singlet.*

S10. Table of metabolite relaxation time T_2 for dataset 2: GM and WM

T2 [ms]	Fitting sum spectra from all subjects		Fitting individual subjects		
	WM	GM	WM	GM	p
Asp, GABA, Glu, Gln, GSH, Gly, GPC, Lac, NAA R, NAAG, PE, Tau	250	203	250 ± 4	205 ± 11	<0.01
Cr / PCr CH_2	144	136	145 ± 11	137 ± 4	>0.05
Cr / PCr CH_3	219	201	220 ± 13	202 ± 7	<0.01
Glc, mI, sI	147	227	149 ± 18	229 ± 23	<0.01
GPC / PCho Trimethyl	268	314	269 ± 18	314 ± 21	<0.01
NAA singlet	400	345	400 ± 0.5	349 ± 29	<0.01

Table S10 – *Results for metabolite relaxation time T_2 in dataset 2 for fitting individual subjects and also the summed data over all subjects, which are in good agreement. P-values, obtained by a paired Mann–Whitney U test, indicate significant differences between GM and WM content for all metabolites except the Cr/PCr CH_2 singlet.*

S11. Repeated measurements for one subject from Dataset 2: Metabolite concentrations and CRLB for GM and WM

Concentration [mM]	Individual fitting of 5 repetitive measurements from one subject		CRLB	
	WM	GM	WM	GM
Asp	1.24 ± 0.34	2.78 ± 0.45	0.16	0.14
Cr	5.00 ± 0.31	6.52 ± 0.16	0.13	0.13
GABA	1.35 ± 0.23	2.17 ± 0.07	0.13	0.11
Glc	3.51 ± 0.53	1.72 ± 0.32	0.12	0.08
Glu	8.01 ± 0.21	11.55 ± 0.28	0.16	0.15
Gln	2.36 ± 0.34	4.35 ± 0.26	0.13	0.12
GSH	1.29 ± 0.12	1.61 ± 0.09	0.06	0.05
Glyc	0.00 ± 0.00	0.55 ± 0.16	0.10	0.08
GPC	1.22 ± 0.09	0.09 ± 0.02	0.04	0.03
Lac	0.53 ± 0.14	0.40 ± 0.21	0.07	0.06
mI	7.64 ± 0.24	5.72 ± 0.24	0.15	0.10
NAA	10.57 ± 0.41	10.03 ± 0.14	0.09	0.08
NAAG	2.75 ± 0.23	2.24 ± 0.11	0.06	0.05
PCr	2.80 ± 0.31	1.58 ± 0.16	0.12	0.11
PCho	0.00 ± 0.00	0.97 ± 0.05	0.07	0.05
PE	2.55 ± 0.32	1.80 ± 0.43	0.14	0.12
sI	0.44 ± 0.07	0.31 ± 0.03	0.03	0.02
Tau	0.04 ± 0.05	1.53 ± 0.17	0.11	0.10

Table S11 – Estimated *metabolite concentrations from individual fits from 5 repeated measurements on the same subject.*

S12. Repeated measurements for one subject from dataset 2: Relaxation times and CRLB for GM and WM

Relaxation times	T_1		T_1 CRLB		T_2		T_2 CRLB	
	WM	GM	WM	GM	WM	GM	WM	GM
Asp, GABA, Glu, Gln, GSH, Gly, GPC, Lac, NAA R, NAAG, PE, Tau	1692 ± 108	1787 ± 67	36.0 ± 4.3	28.8 ± 3.0	250	208 ± 7	6.3 ± 0.7	3.4 ± 0.4
Cr / PCr CH_2	1252 ± 75	1216 ± 45	25.4 ± 1.5	20.8 ± 1.4	150 ± 7	140 ± 3	3.5 ± 0.4	2.2 ± 0.2
Cr / PCr CH_3	1879 ± 150	1631 ± 48	33.1 ± 5.1	23.7 ± 2.5	218 ± 16	205 ± 5	4.4 ± 0.9	2.7 ± 0.3
Glc, mI, sI	1498 ± 131	1375 ± 54	23.8 ± 2.5	22.2 ± 1.8	150 ± 17	249 ± 31	5.3 ± 1.1	9.4 ± 2.0
GPC / PCho Trimethyl	1516 ± 117	1419 ± 47	26.3 ± 2.6	37.1 ±2.9	266 ± 12	320 ± 8	6.3 ± 0.5	9.7 ± 0.8
NAA singlet	1862 ± 68	1983 ± 26	25.9 ± 1.9	27.3 ± 2.0	400	370 ± 7	6.6 ± 0.5	5.0 ± 0.4

Table S12 – *Estimated relaxation times and CRLB from individual fits for 5 repeated measurements on the same subject.*